

***Geoelectrical
and electromagnetic method
APPLIED Geophysics 2020
Edited by G. Pethő***

Short history

- **Faraday (1831):** induction law, introduction of dielectric constant
- **Maxwell (1861-62):** foundation of classical electrodynamics
- **Schlumberger (1912):** first geoelectrical measurement with artificial source
- **Sunberg (1923) :** induction method, horizontal loop array
- **Stern (1929):** ice thickness measurement in the Alps with georadar
- **Cagniard, Tichonov, Kato, Kikuchi, Rikitake (in the 50-s):** development of magnetotellurics
- **Krajev (1941):** the idea of artificial EM frequency sounding
- **Vanjan(1965), Keller(1968):** development of FEM
- **Fokin (1971), Kaufmann, Keller (in the 80-s):** development of TEM
- **Semenov (1978), Goldman (1994):** Magnetic resonance sounding

Goelectrical methods; 1st part

SUMMARY of the GEOELECTRICAL METHODS

The electrical properties of the sub-surface can be explored by either goelectrical or electromagnetic methods. In the case of goelectrical methods we apply DC in theory, and low frequency current in practice. The DC natural source field method is called self-potential (SP) method. The occurrence of self-potential may be due to electro-filtration, concentration difference (diffusion), contact potential and mineral potentials. The object of vertical electrical sounding is to determine the variation of electrical resistivity with depth. The current penetration can be controlled by the geometry of the array. The shape of the sounding curve reflects the resistivity variation with depth. However, widely different resistivity distribution may lead to apparent resistivity sounding curves which cannot be distinguished in practice. For this reason the principle of equivalence and layer suppression introduces ambiguity in the interpretation.

The types of electrical conduction

Metallic conduction: in the case of native metals due to the large amount of valence electrons (copper, silver, gold, graphite with resistivity of 10^{-8} ohmm)

Electronic semiconduction: most sulfides and oxides with very few valence electrons and their number increases with temperature increase (galena, ilmenite, pyrite, magnetite with resistivity of 10^{-6} - 10^4 ohmm)

Electrolytic conduction can be either solid electrolytes (ionic crystals) or electrolyte water solutions. Most rock forming minerals (quartz etc.) act as solid electrolytes, where the conduction is due to the motion of ions through the crystal lattice (with resistivity of 10^3 - 10^{14} ohmm). In water saturated formations the electrical conductivity of pore water is dominant over the matrix conductivity.

Insulators with dielectric polarisation.

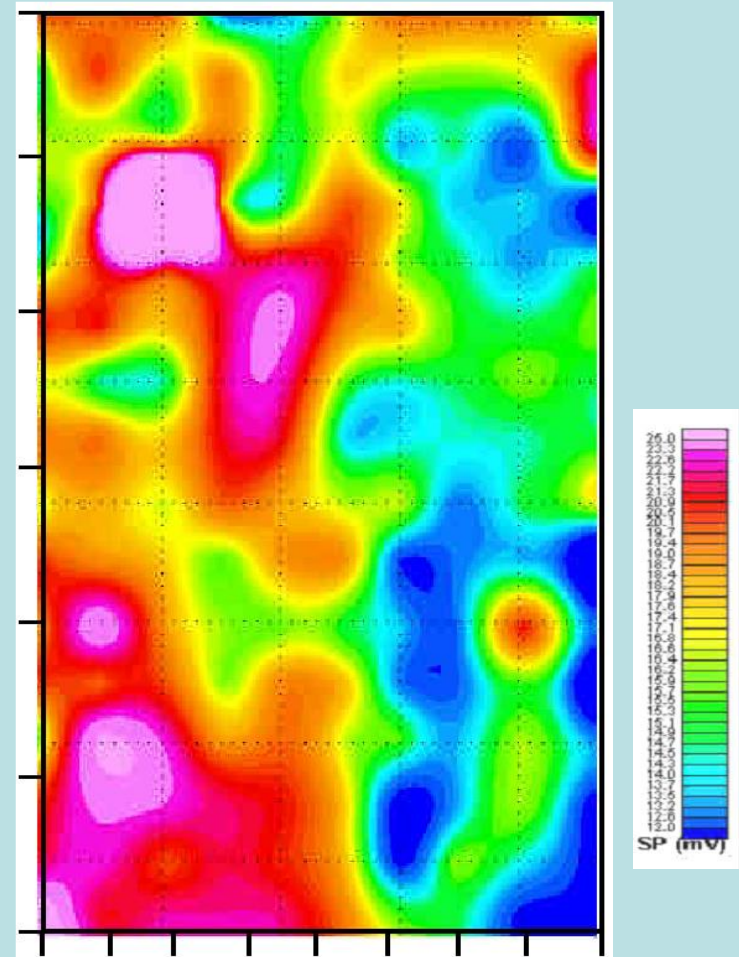
$$E = \frac{\varepsilon \rho \zeta}{4\pi \eta} p$$

PS filtration potential

E denotes the electric field between the two ends of the cylinder with small diameter, p stands for the pressure gradient, ε dielectric permittivity, ρ resistivity, η refers to dynamic viscosity. ζ parameter denotes the zeta potential depending on the chemical composition of the fluid and that of the pore wall.

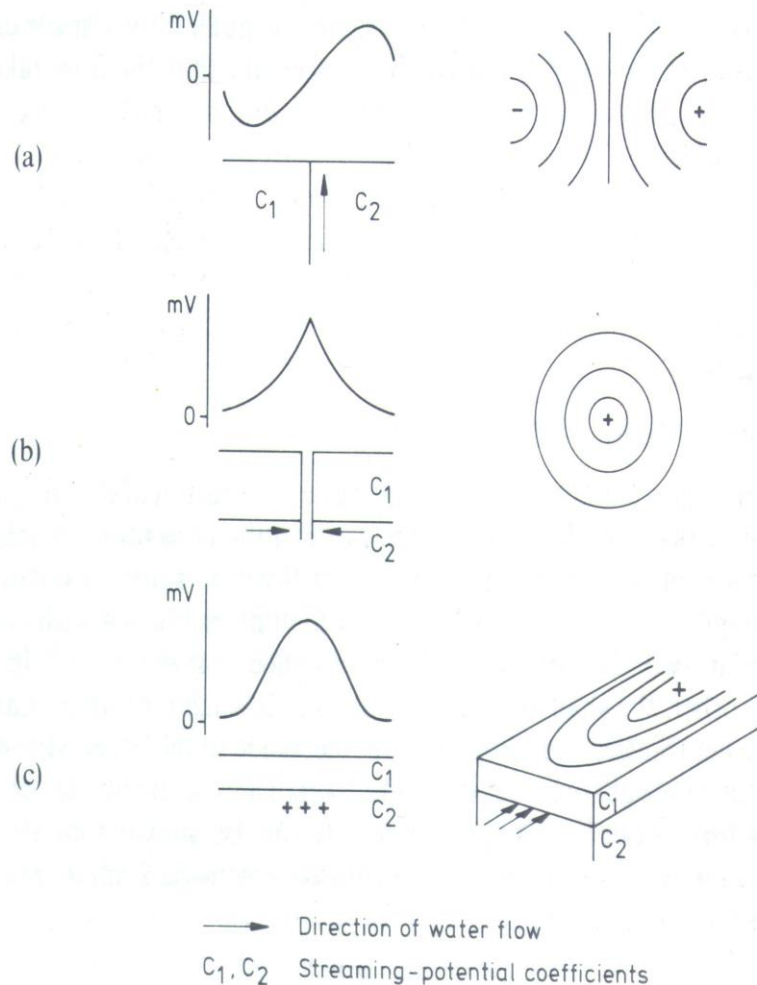
Negative ions of the fluid are absorbed by the wall, the relative occurrence of the positive ions increases, the velocities of the ions are different.

Streaming potential coefficient -for any medium- can be defined as the ratio of the electric field and the pressure gradient.



Gamal et al.

PS Filtration potential



If the direction of water flow is parallel to the boundary, then the measured filtration potential is greater than in other cases.

Idealized electrofiltration SP (profiles and maps) on some flow models. After [50]. (a) Vertical boundary; (b) pumping from a well; (c) horizontal boundary flow.

PARASNIS (1986)

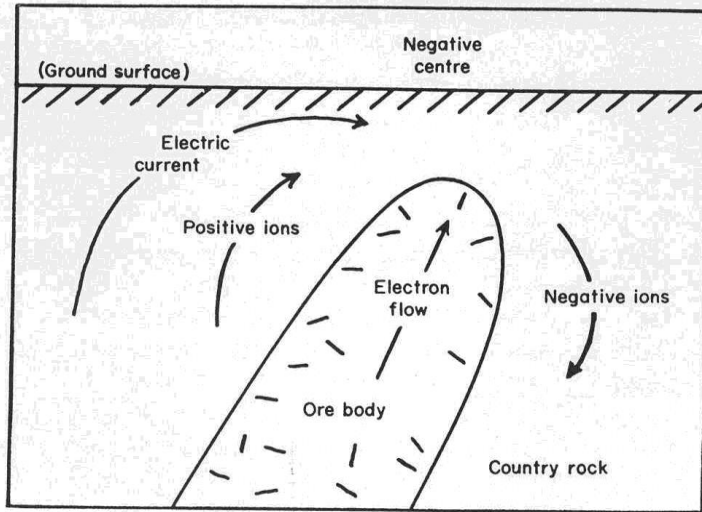
PS Electrochemical potential

It is the sum of the diffusion and Nernst potential. The diffusion potential develops in the presence of two solutions in contact. Because the two solutions have different ion concentrations, an ion diffusion rates from a more concentrated to a more dilute solution. The ion mobility depends on the ion diameter. This liquid-junction potential is produced at the contact of the two solutions. Nernst potential develops if two identical metal electrodes are immersed in solutions with different concentrations.

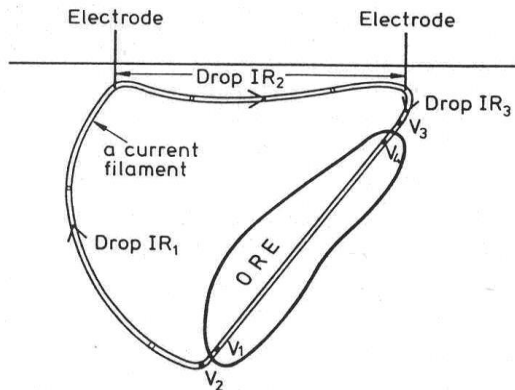
$$E_D = \frac{u - v}{u + v} \frac{RT}{nF} \ln \frac{C_1}{C_2}$$

$$E_N = -\frac{RT}{nF} \ln \frac{C_1}{C_2}$$

PS Mineralization potential



Current and ion flow in the vicinity of an ore body.

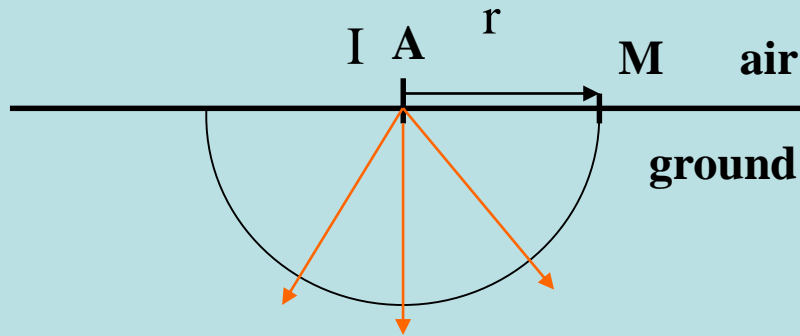


Potential drops in SP observations.

Natural voltages associated with oxide or sulphide deposits. They develop due to the electrochemical and electrolytic contact potentials. The electrolytic contact potential is due to dissimilar metals when immersed in an electrolyte. Kilty (1984) did not assume electrochemical equilibrium, he applied Kirhoff's law to characterize the resultant mineralization. The potential difference IR_2 can be measured on the surface.

$$(V_1 - V_2) + IR_1 + IR_2 + IR_3 + (V_3 - V_4) + V_4 - V_1 = 0$$

Potential due to a point source on the surface



Over a homogeneous half-space at a distance r from the transmitter electrode the potential can be determined from the current density (j). In the figure red arrows correspond to the current density vectors which are perpendicular to the equipotential surface (black hemisphere). In the knowledge of the current (I) introduced into the ground and with the use of differential Ohm's law it can be written:

$$\vec{j} = \frac{I}{2\pi r^2} = \sigma \vec{E} = \sigma(-grad U) = \sigma\left(-\frac{\partial U}{\partial r}\right)$$

After integration the value of the potential:

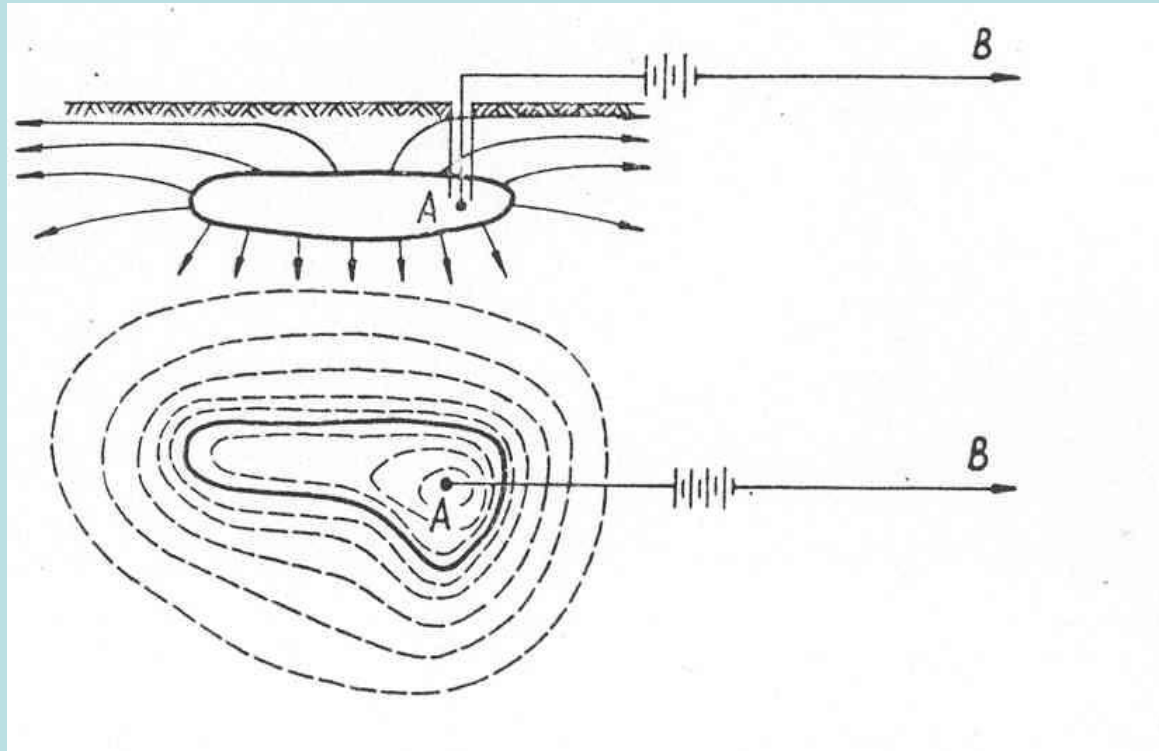
$$U = \frac{\rho I}{2\pi r} + C$$

If $r \rightarrow \infty$, then U tends to zero: $U(r) = \frac{\rho I}{2\pi r}$

In the case of a homogeneous space:

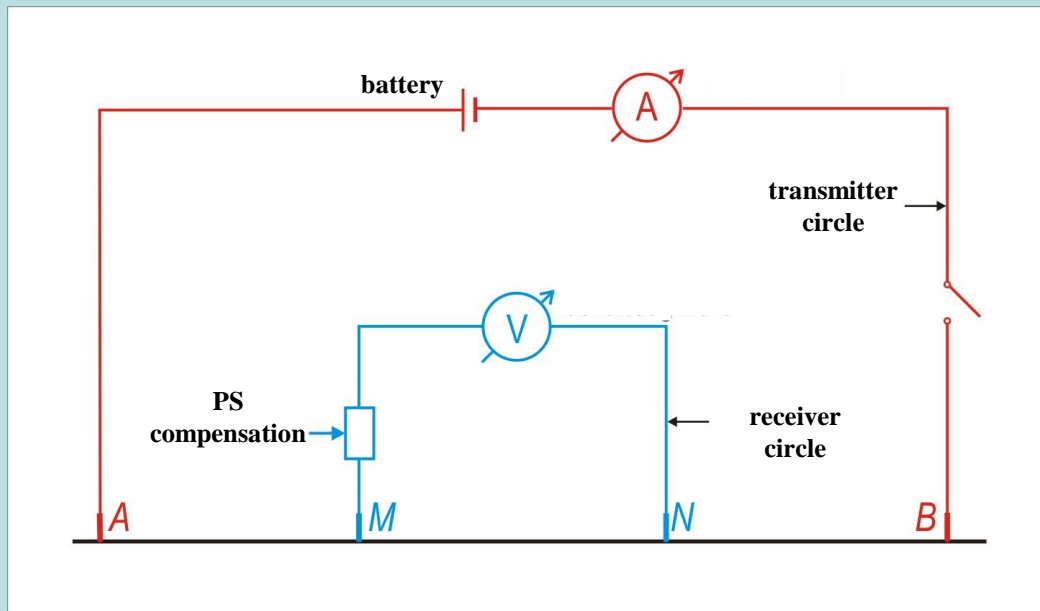
$$U(r) = \frac{\rho I}{4\pi r}$$

Mise-a-la-masse method



The aim is to map the mineral deposit with high conductivity. One transmitter electrode is positioned in a conducting material (ore dyke, streaming water) by means of a borehole, the other transmitter electrode is a great distance away. Actually the intersections of the equipotential surfaces with the surface are determined by the potential electrodes.

Resistivity measurement



$$U_M = \frac{\rho I}{2\pi AM}$$

$$U_N = \frac{\rho I}{2\pi AN}$$

$$\Delta U_{MN} = \frac{\rho I}{2\pi AM} - \frac{\rho I}{2\pi AN}$$

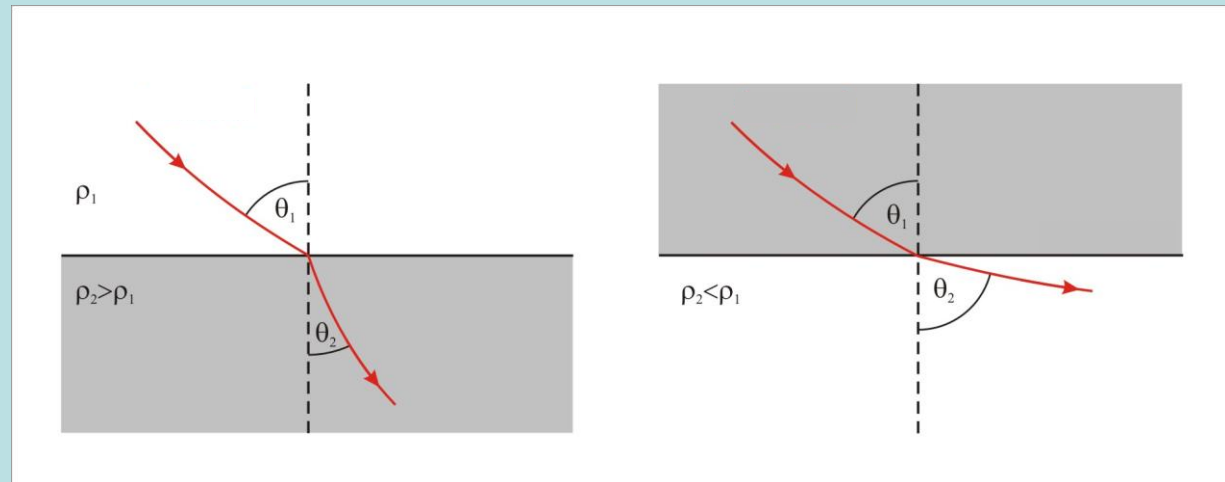
$$\Delta U_{MN} = \frac{-\rho I}{2\pi BM} + \frac{\rho I}{2\pi BN}$$

$$\Delta U_{MN} = \frac{\rho I}{2\pi} \left(\frac{1}{AM} - \frac{1}{BM} - \frac{1}{AN} + \frac{1}{BN} \right)$$

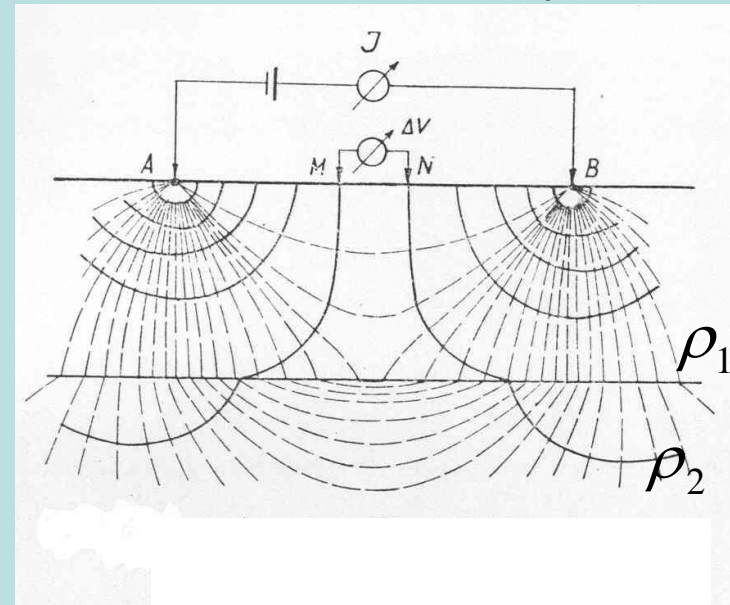
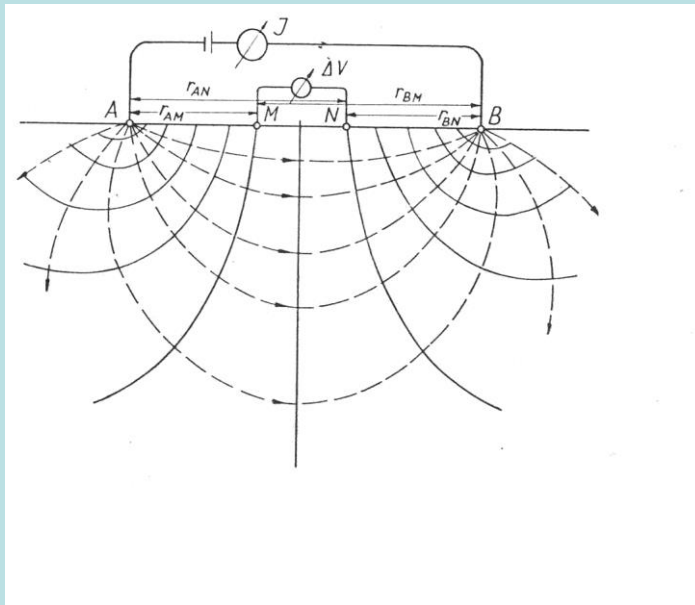
$$\rho = \frac{2\pi}{\left(\frac{1}{AM} - \frac{1}{BM} - \frac{1}{AN} + \frac{1}{BN} \right)} \frac{\Delta U_{MN}}{I}$$

$$\rho = k \frac{\Delta U_{MN}}{I}$$

$$\frac{\operatorname{tg} \theta_1}{\operatorname{tg} \theta_2} = \frac{\rho_2}{\rho_1}$$



the behaviour of current lines at horizontal boundary

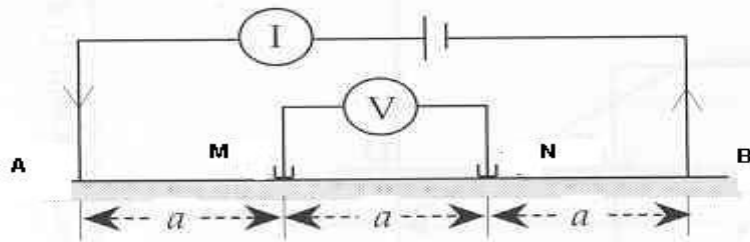


Distribution of current lines and equipotential lines for homogeneous half-space and for a two-layer half-space when $\rho_2 < \rho_1$

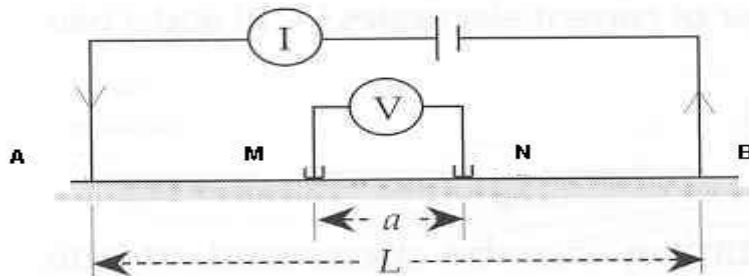
(Renner et. al 1970)

Vertical Electric Sounding (VES)

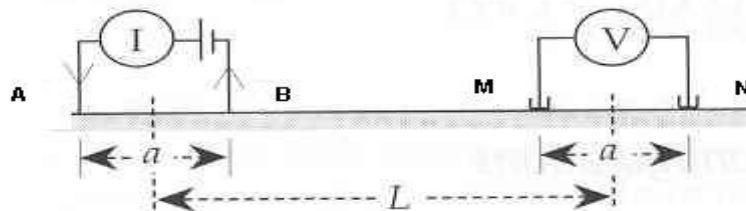
(a) Wenner



(b) Schlumberger

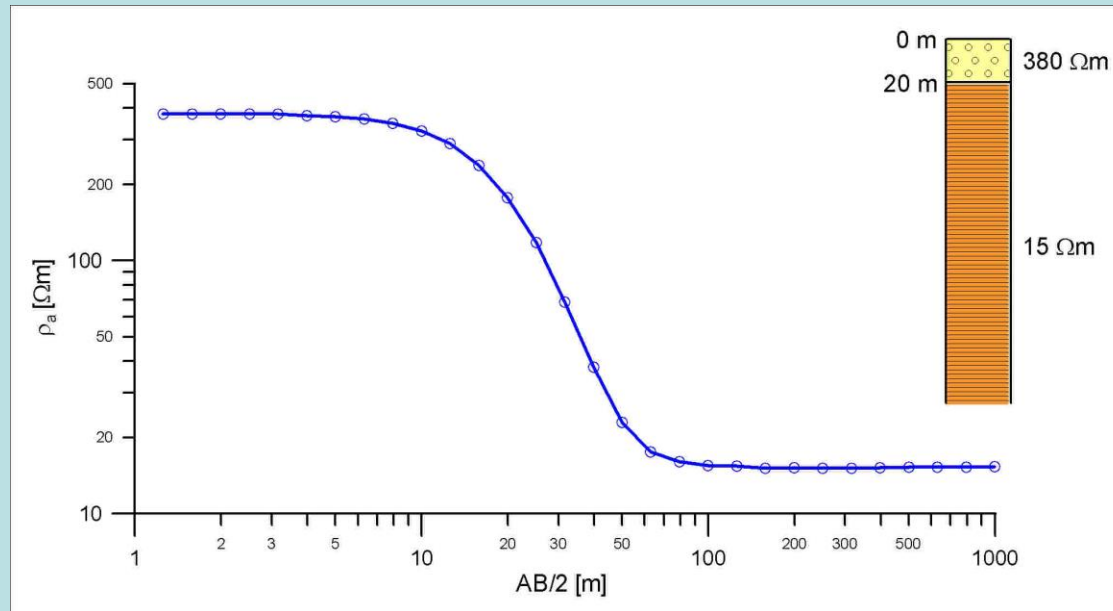


(c) Double-dipole **Dipole-dipole**

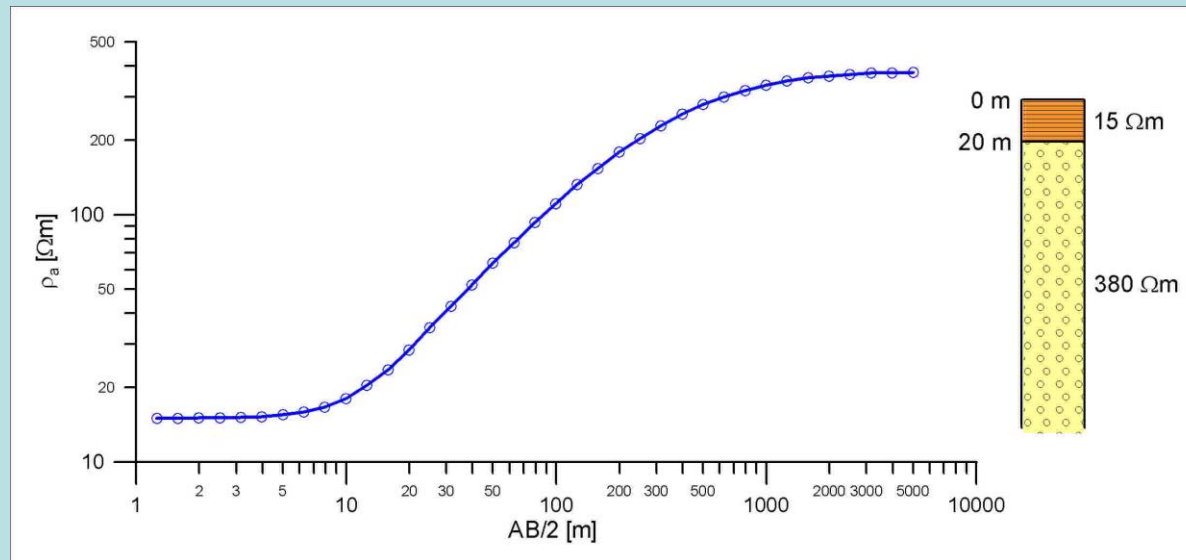


Exploration depth can be governed by the geometry of the array(s). The larger the value of a (for Wenner configuration) or the value of L (for Schlumberger and dipole-dipole arrays) is, the greater the penetration depth will be.

VES app. resistivity curves

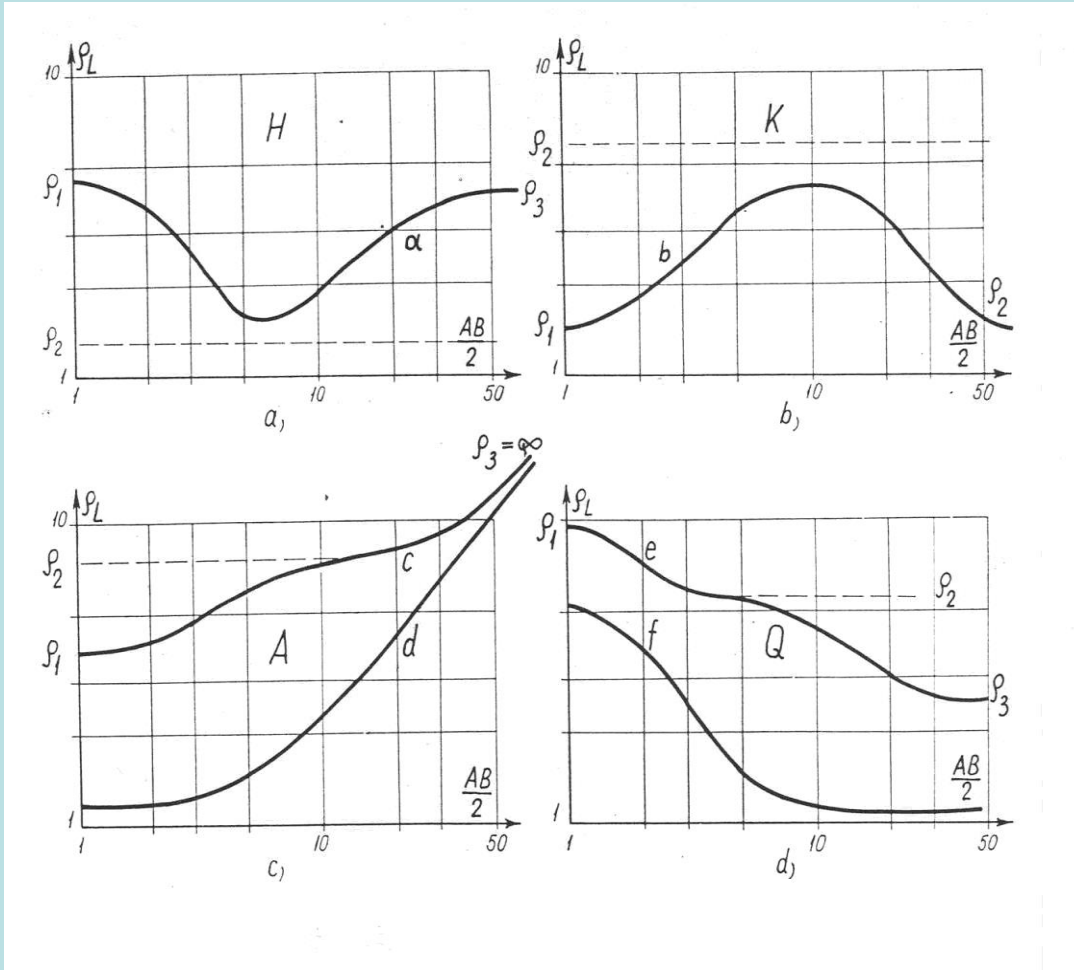


$$\rho_2 < \rho_1$$



$$\rho_2 > \rho_1$$

VES



$$\rho_1 > \rho_2 < \rho_3 \quad \mathbf{H}$$

$$\rho_1 < \rho_2 > \rho_3 \quad \mathbf{K}$$

$$\rho_1 < \rho_2 < \rho_3 \quad \mathbf{A}$$

$$\rho_1 > \rho_2 > \rho_3 \quad \mathbf{Q}$$

There are four types of VES apparent resistivity sounding curves if the half-space consists of three layers.

VES, S-type of equivalence

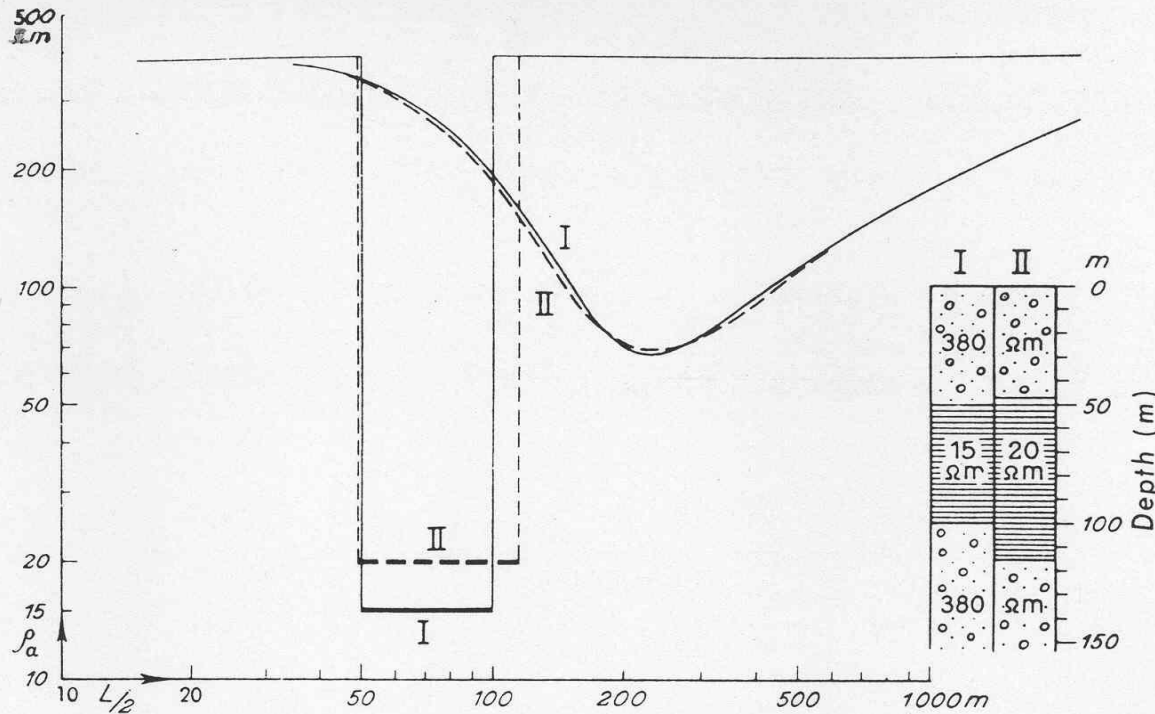
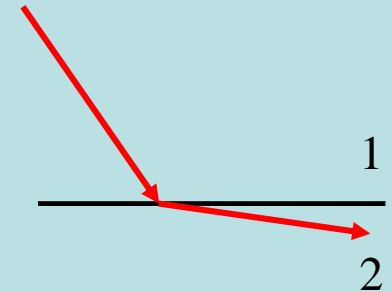


Illustration of the principle of equivalence for a conductive bed lying between two resistive beds. In the example shown, the resistivity curves are practically the same for two situations: (I) middle layer of resistivity 15 Ωm and thickness 50 m, or (II) resistivity 20 Ωm and thickness 66 m. (After Bentz, 1961.)

H-type of layering

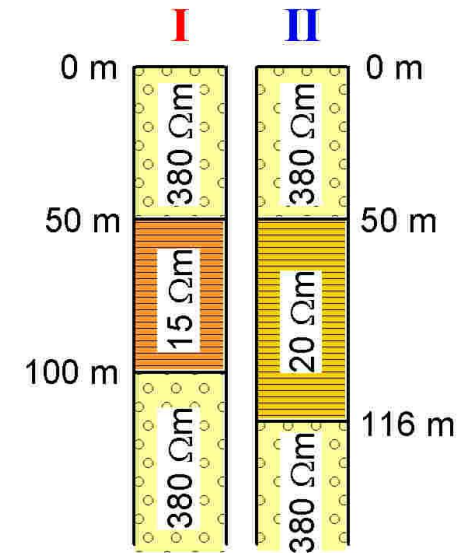
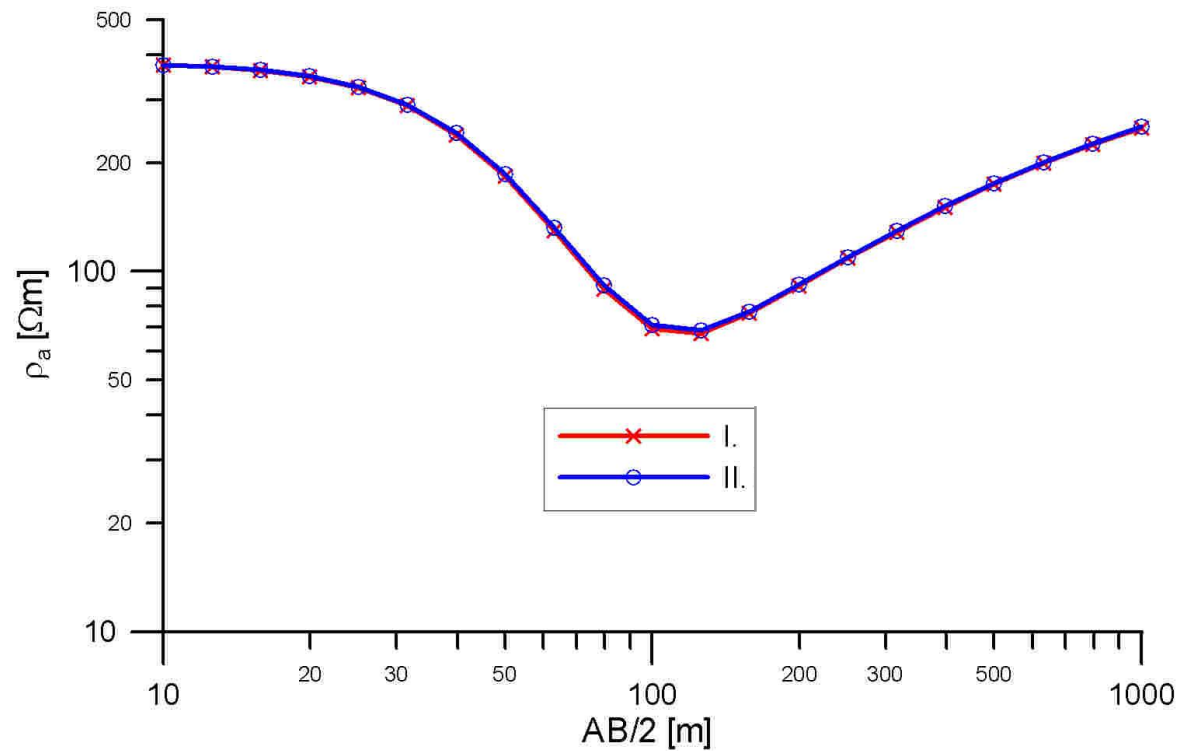
$$\rho_1 > \rho_2 < \rho_3$$



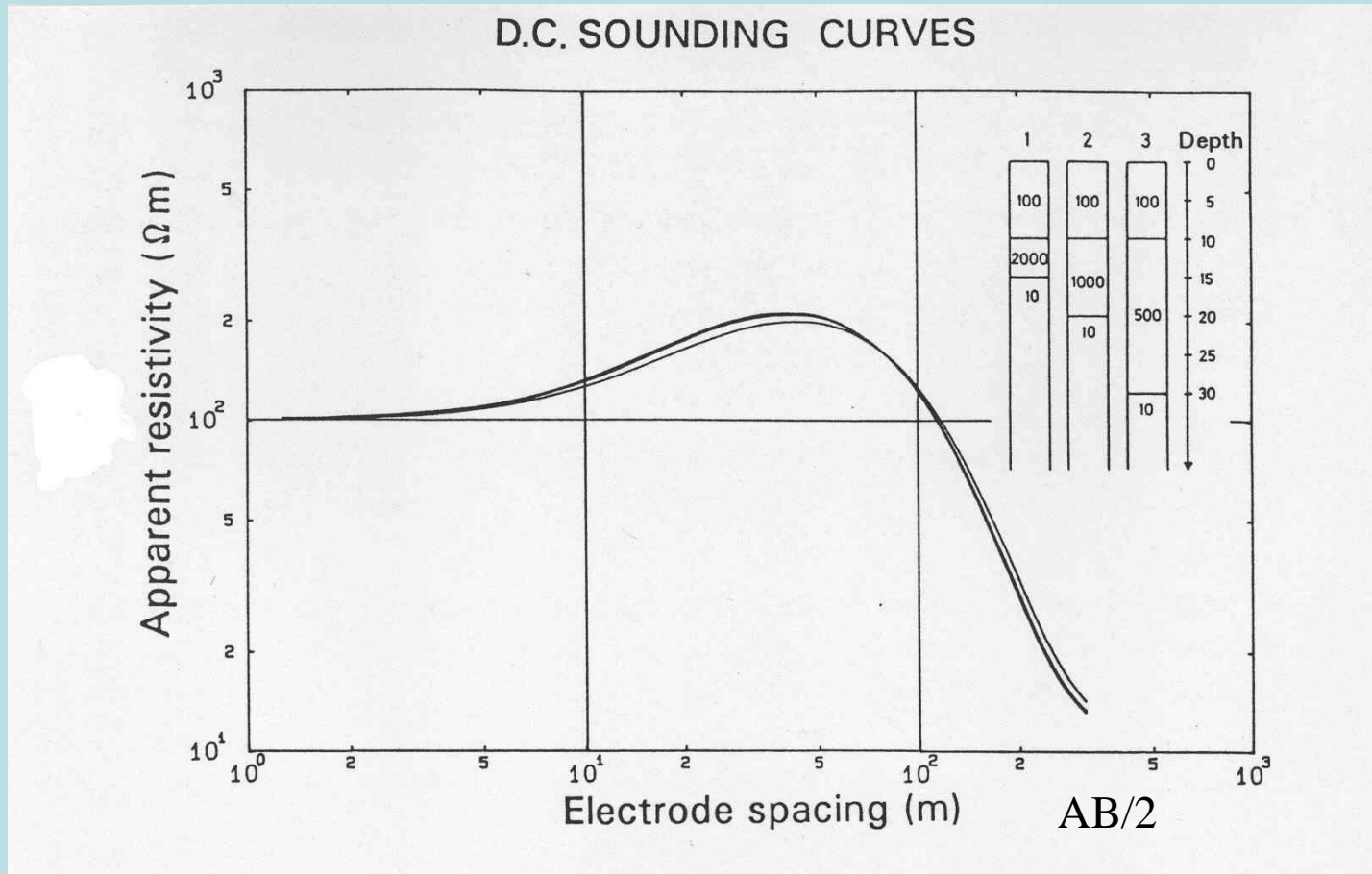
$$S_2 = h_2 / \rho_2$$

There is no difference in the apparent resistivity sounding curves for the two cases if the longitudinal conductances (S_2) are the same for the sandwiched layers.

VES, S-type of equivalence

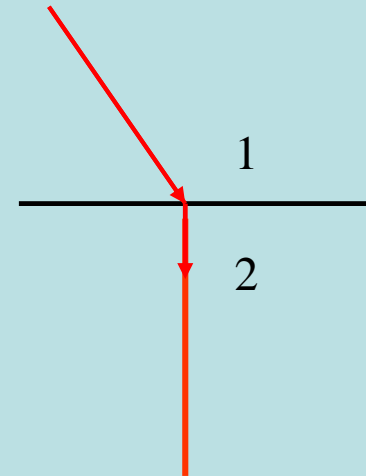


VES, T-type of equivalence



K

$$\rho_1 \langle \rho_2 \rangle \rho_3$$

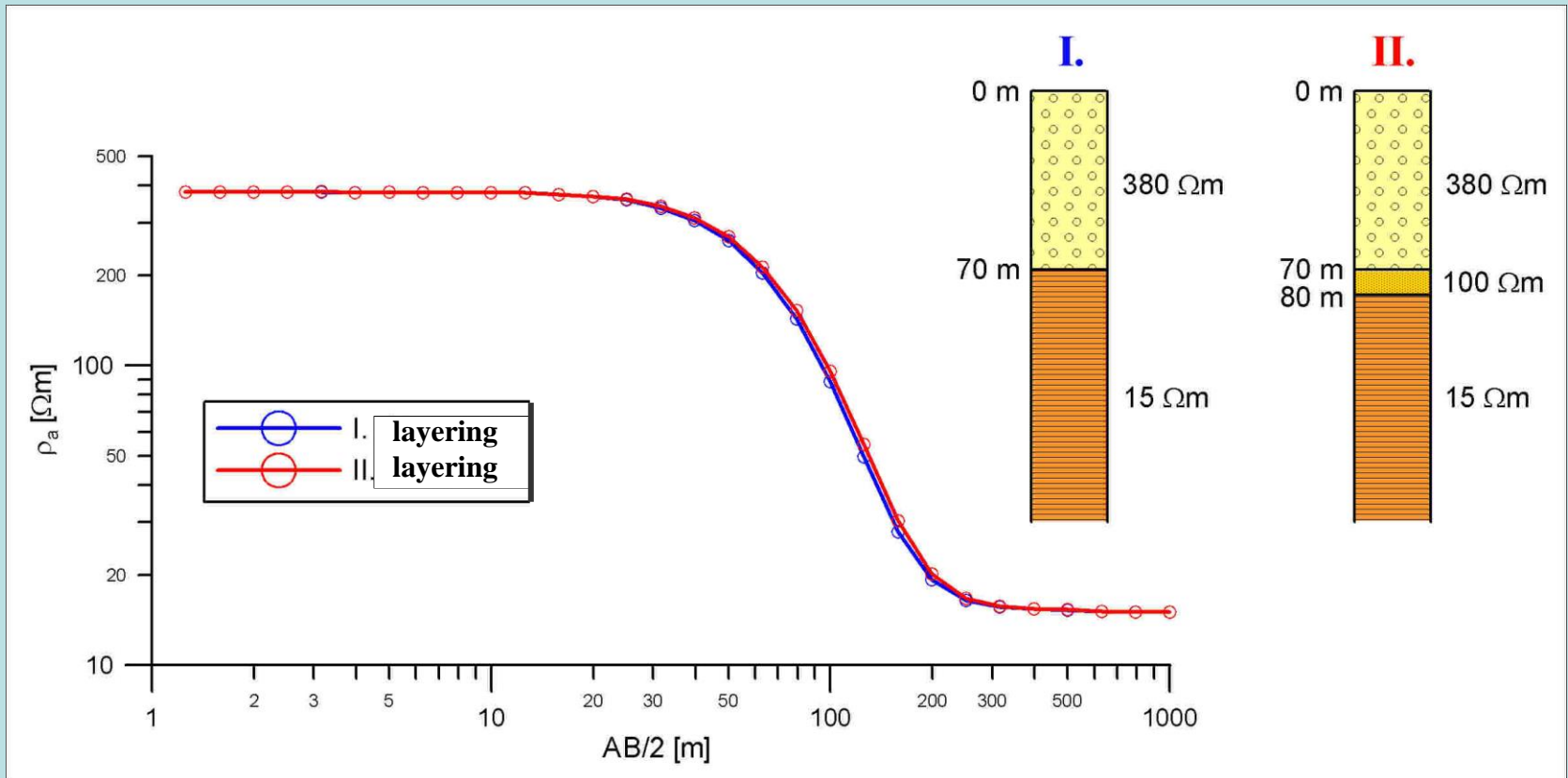


$$T_2 = \rho_2 h_2$$

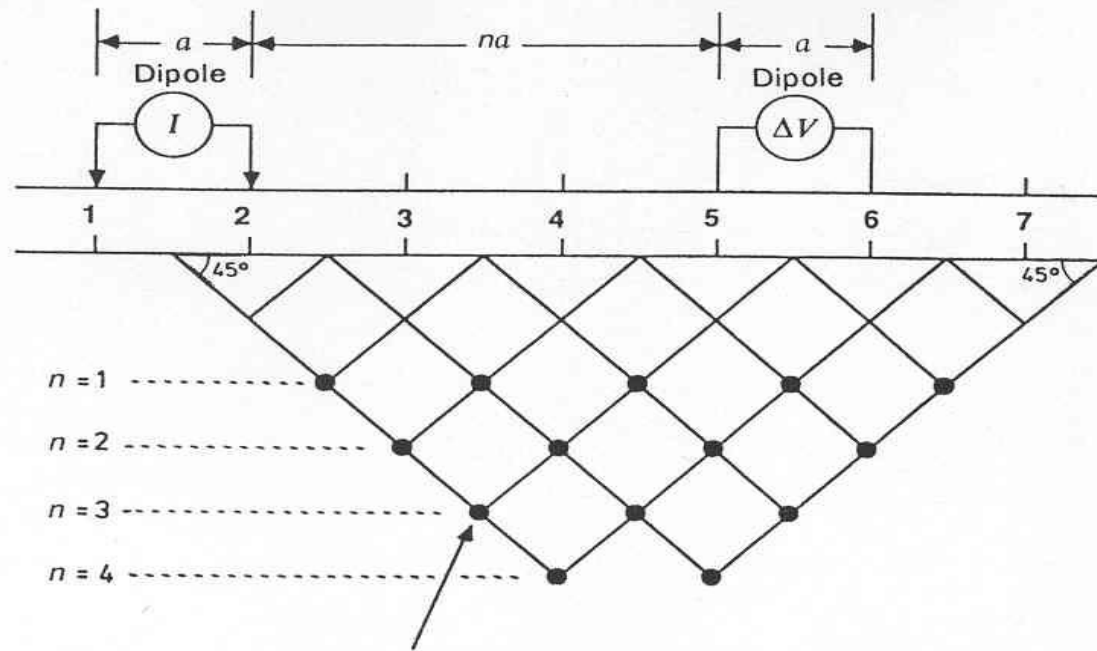
There is no difference in the apparent resistivity sounding curves for the cases if the transverse resistances (T_2) are the same for the sandwiched layers.

(Sharma, 1997)

Layer Suppression



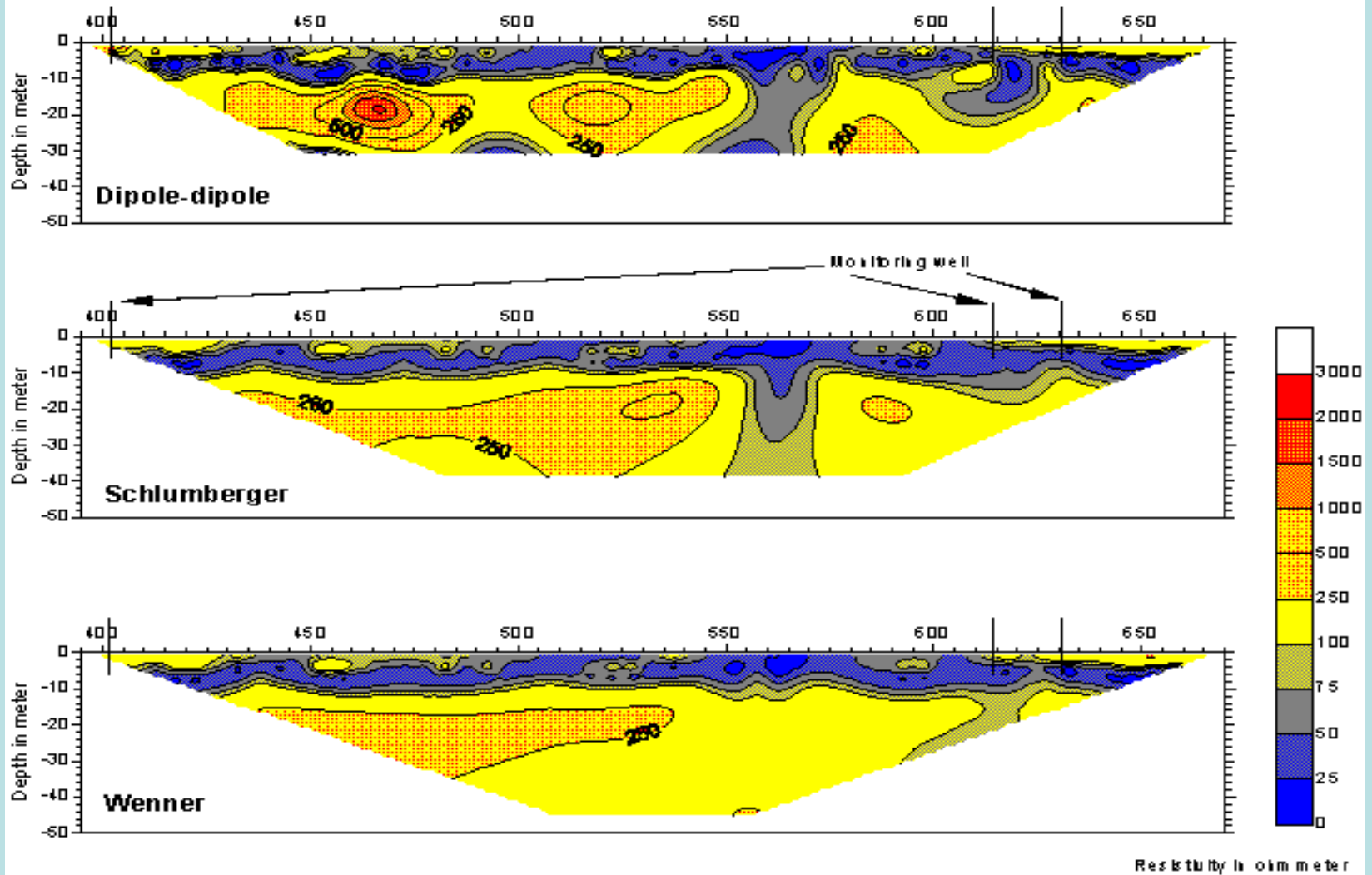
It is impossible to recognize the effect of the second layer, because it is thin and it has a transitional resistivity value.



Plot value of app. resistivity at 1-2, 5-6

Method of plotting dipole-dipole apparent resistivity data in a pseudosection. n represents the relative spacing between the current and potential dipoles.

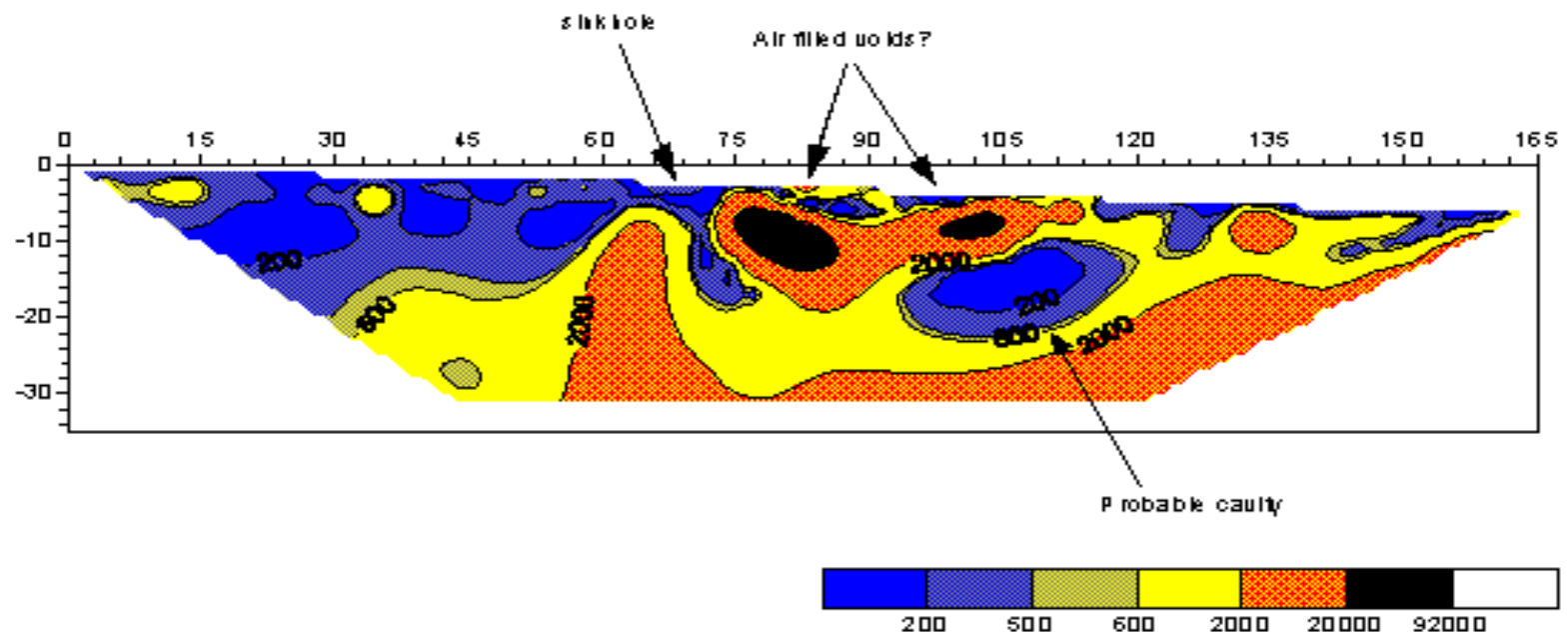
Amistad October 10, 1996



Sinkhole in karst region

Pellissippi Parkway

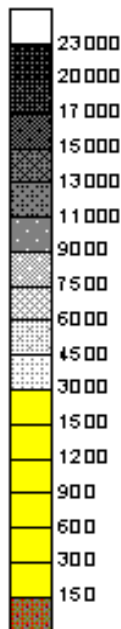
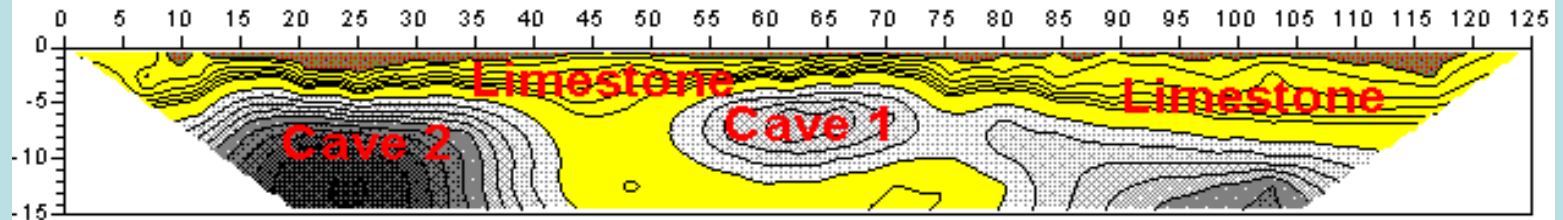
Objective: Locate sinkhole in karst area
Survey date: October 15, 1996
Method: Dipole-dipole resistivity
Unit: Meter and Ohmmeter
Instrument: Sting/Swift, 56 electrodes at 3 meter spacing



Tel: +1 (512) 335-3338
Fax: +1 (512) 258-9958
e-mail: sales@agiusa.com

Courtesy of Dr. Barry Beck P.E., LaMoravia, Knoxville, Tennessee

The Sting Cave



Cave 2, the Sting cave, was detected during a test measurement over a previously known cave, Cave 1. This cave shows lower resistivity than the Sting cave as Cave 1 has floor to ceiling columns which act as current conduits. The Sting cave does not have any columns. Both caves were confirmed by drilling large diameter, 24 inch, entrance holes. Depth to ceiling for Cave 1 is 1.8 m, for Cave 2 is 7.3 m.

The resistivity section above was calculated from the apparent resistivity data using the RES2DINV automatic inversion software. The graphical presentation was made using the Surfer for Windows software.

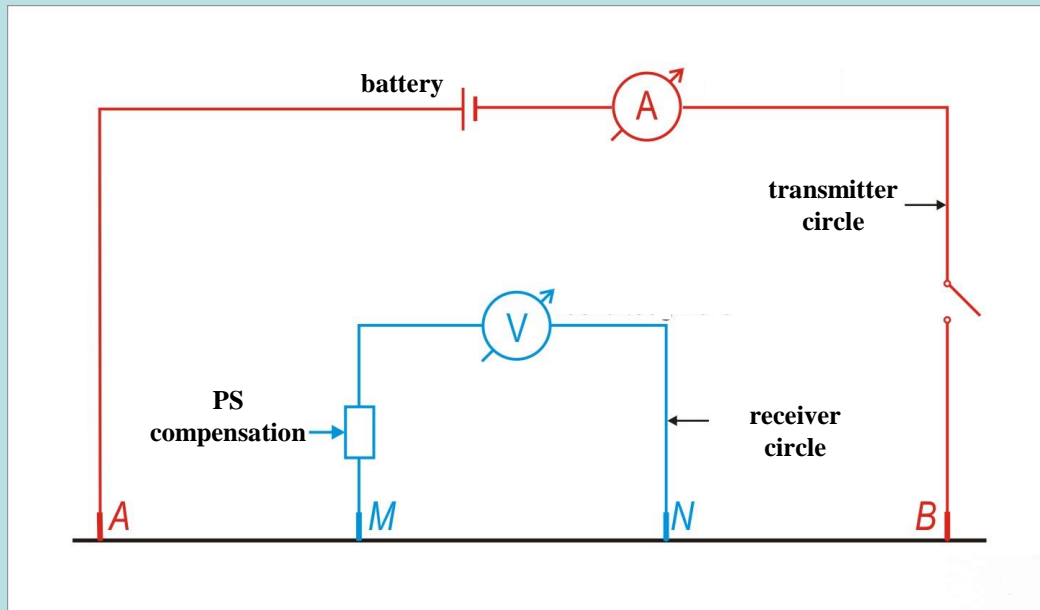
Survey date: October 29, 1994
 Method: Dipole-dipole resistivity (dipole 4.6 m, n=8)
 Unit: Meter and ohmmeter
 Instrument: Sting/Swift, 28 electrodes at 4.6 m spacing
 Survey time: Set-up and take down 1 hour (2 man crew)
 Data acquisition 40 min

Courtesy of Gasch & Associates, Sacramento California

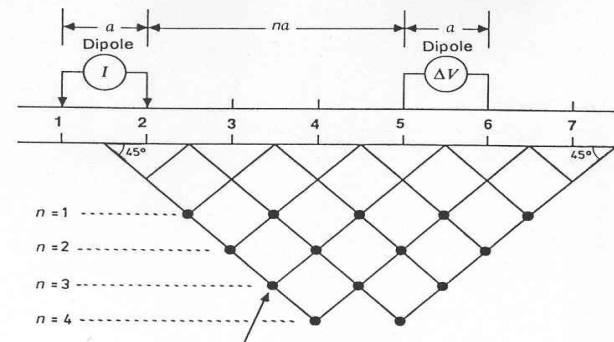


Tel: +1 (512) 335-3338
 Fax: +1 (512) 258-5658
 e-mail: sales@agiusa.com

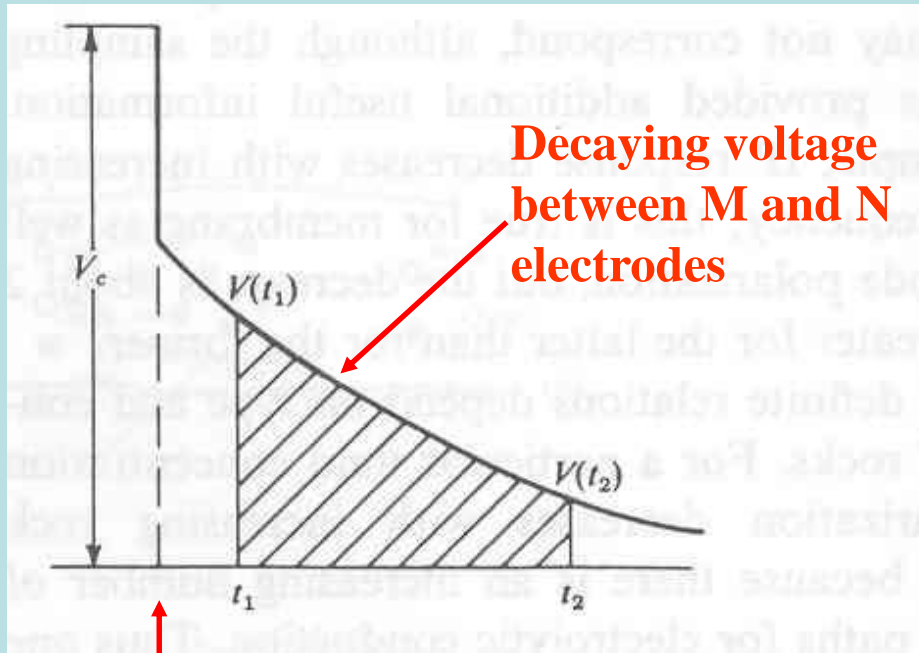
Induced polarization (IP) in time domain



The same arrays are used as in the case of resistivity measurement.



Induced polarization (IP) in time domain

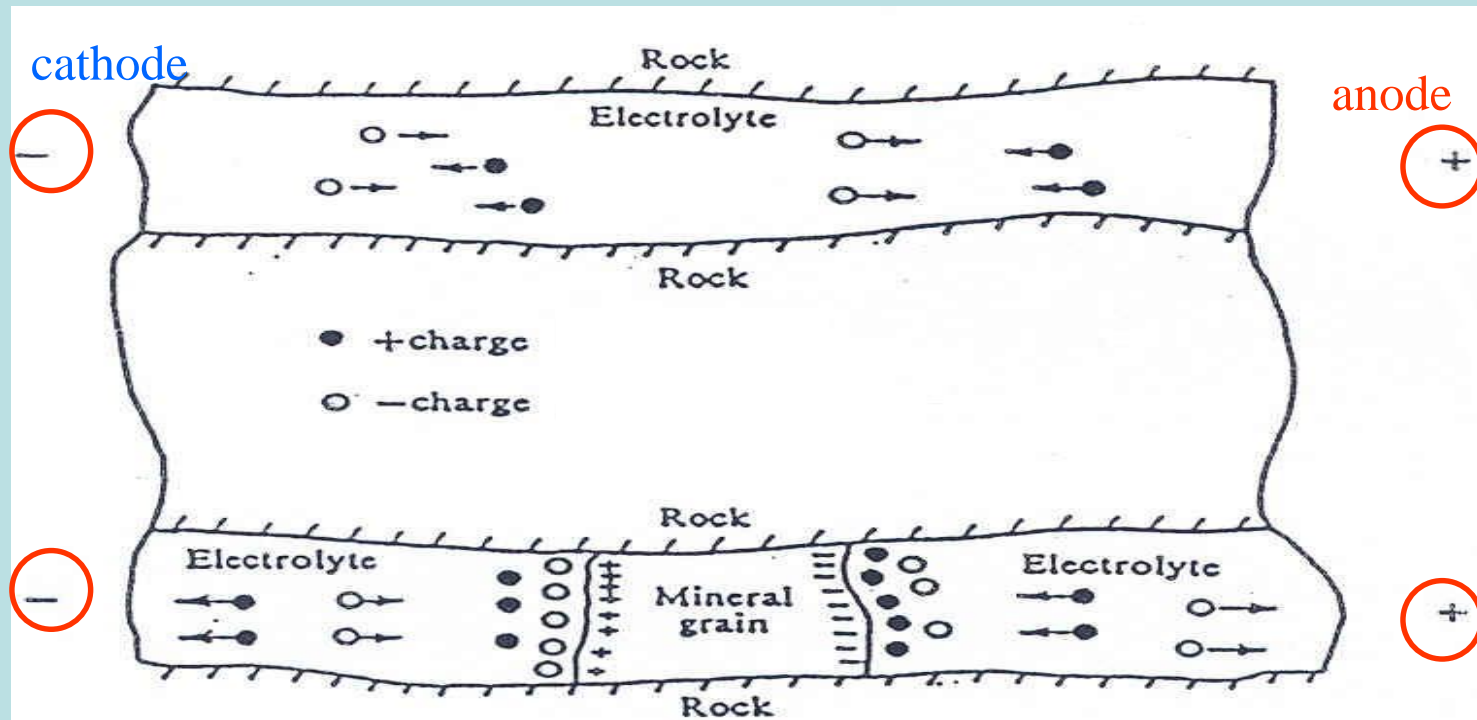


The time of switching off

In certain situations (disseminated ore grains, the presence of clay) after switching off the transmitter current a decaying voltage can be observed between the potential electrodes. This induced polarization can be investigated in time and in frequency domain. This figure refers to the time domain observation. The most important parameter is the chargeability (M):

$$M = \frac{\int_{t_1}^{t_2} V(t) dt}{V_c}$$

Electrode polarization

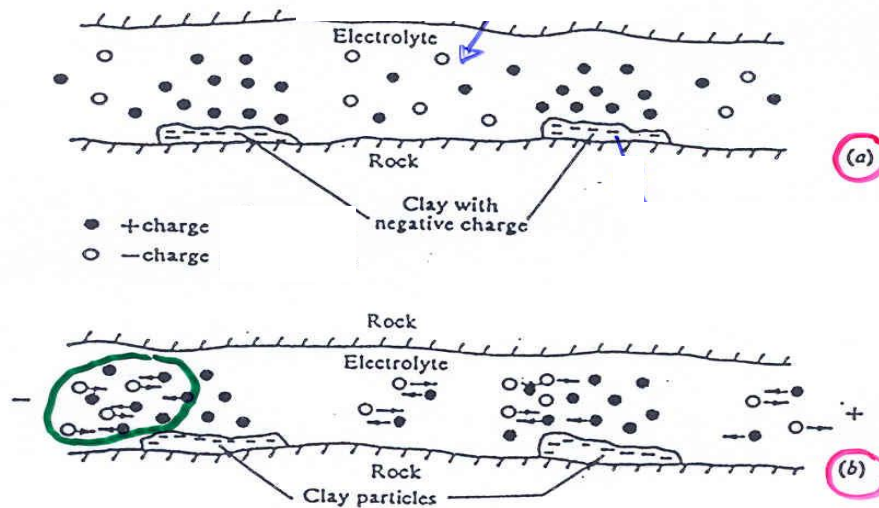


(Telford et. al., 1993: Applied Geophysics)

Current flow must be both electrolytic and electronic as well. At the boundary separating the mineral grain and the solution an electron exchange takes place between the metal and the ion in the solution. The external voltage maintains the pileup of ions at the boundary because the current flow in the solution is much slower than in the mineral grain. When the current is switched off, the residual voltage decays as the ions diffuse back to their equilibrium state. This process can be observed in time domain measurement.

Membrane polarization

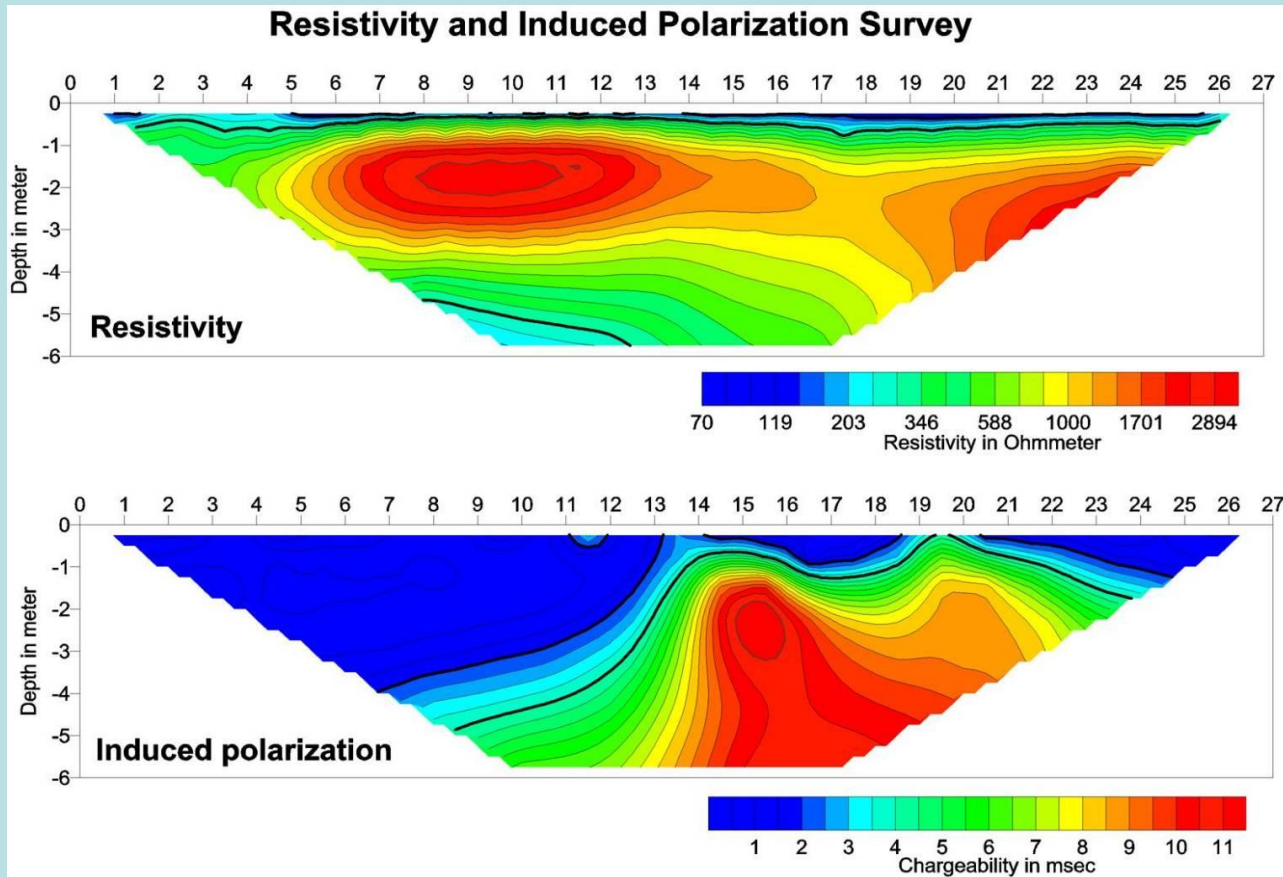
(Telford et. al., 1993: Applied Geophysics)



a: distribution of ions in a pore with electrolyte and membranes without external voltage. b: membrane polarization effect in a porous sandstone due to an external voltage. Even in the shortage of the applied DC voltage the surface of the clay particles attract positive ions of the electrolyte. Due to the applied DC voltage the negative ions will accumulate over the interface of the clay particles closer to the cathode, creating an ion abundant zone opposite to the right part of the membrane (in this case) and the other end of the pore (on the anode side). After switching off, the residual voltage decays as the ions diffuse back to their equilibrium state.

Induced polarization, IP

Resistivity and chargeability over a karstic limestone area.



Objective: To investigate a karstic limestone area using resistivity and induced polarization
Survey date: October 21, 1999
Survey site: Austin, Texas
Electrode array: Schlumberger
Instrument: Sting/Swift, 28 stainless steel electrodes at 1 meter spacing
Units: Meter, Ohmmeter and msec

AGI Advanced Geosciences, Inc.

Tel: +1 (512) 335-3338
Fax: +1 (512) 258-9958
E-mail: sales@agiusa.com
Web site: <http://www.agiusa.com>

**Observations over known CH reservoirs collected
from 16 companies by ZONGE Research Co. 1984.**

occurrence	conductivity increase	great resistivity	increase in chargeability
frequent	36%	0%	45%
occasional	45%	45%	55%
rare	19%	55%	0%

Induced polarization (IP) in frequency domain

If low frequency AC source is used for resistivity measurement, it can be observed that the resistivity decreases as the frequency is increased. The reason of it is that the capacitance of the ground inhibits the passage of direct currents, but transmits alternating currents. The greater the applied frequency is, the less the resistivity will be. In practice two measurements are made at one station at two frequencies. From these values the percentage frequency effect can be determined. If the transmitter frequencies are 0.1 Hz and 10Hz, the PFE is defined as

$$PFE = \frac{\rho_{0.1} - \rho_{10}}{\rho_{10}} 100\%$$

Geophysical EM methods; 2nd part

SUMMARY of the GEOPHYSICAL ELECTROMAGNETIC METHODS

The electromagnetic methods may utilize natural (MT method) or artificial source field.

The latter one (controlled source) may be divided fundamentally into near-field and far field methods based upon the relationship between transmitter-receiver distance and wavelength (in frequency domain, FEM) or transmitter-receiver distance and diffusion depth (in time domain, TEM).

The (artificial) source field may be excited by grounded dipole or by induction. The measured physical parameters are the EM field components and the phase shift between them. From these expressions the apparent resistivity can be derived. The penetration depth of the EM field from the source field is characterized by the skin depth (FEM) or by the diffusion depth (TEM).

Classification of EM methods

On the basis of source they can be either
natural or artificial.

Artificial methods are called controlled source methods as well.

Controlled source methods can be

inductive	conductive
time domain	frequency domain
near field	transitional far field zone

Magnetosphere of the Earth

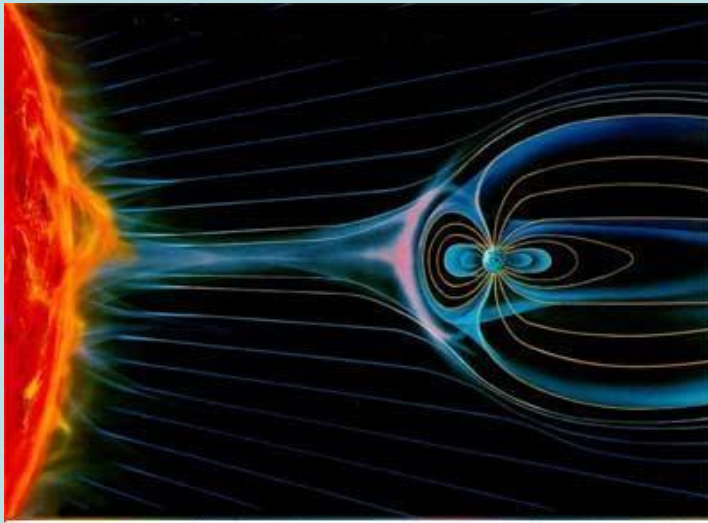
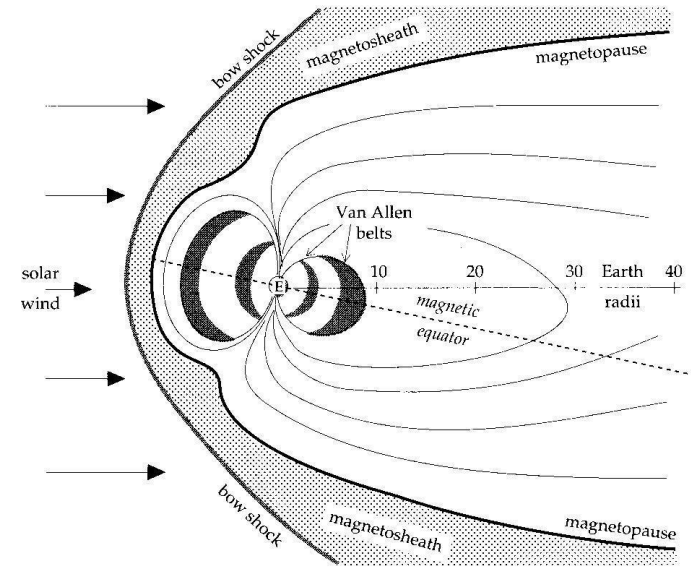
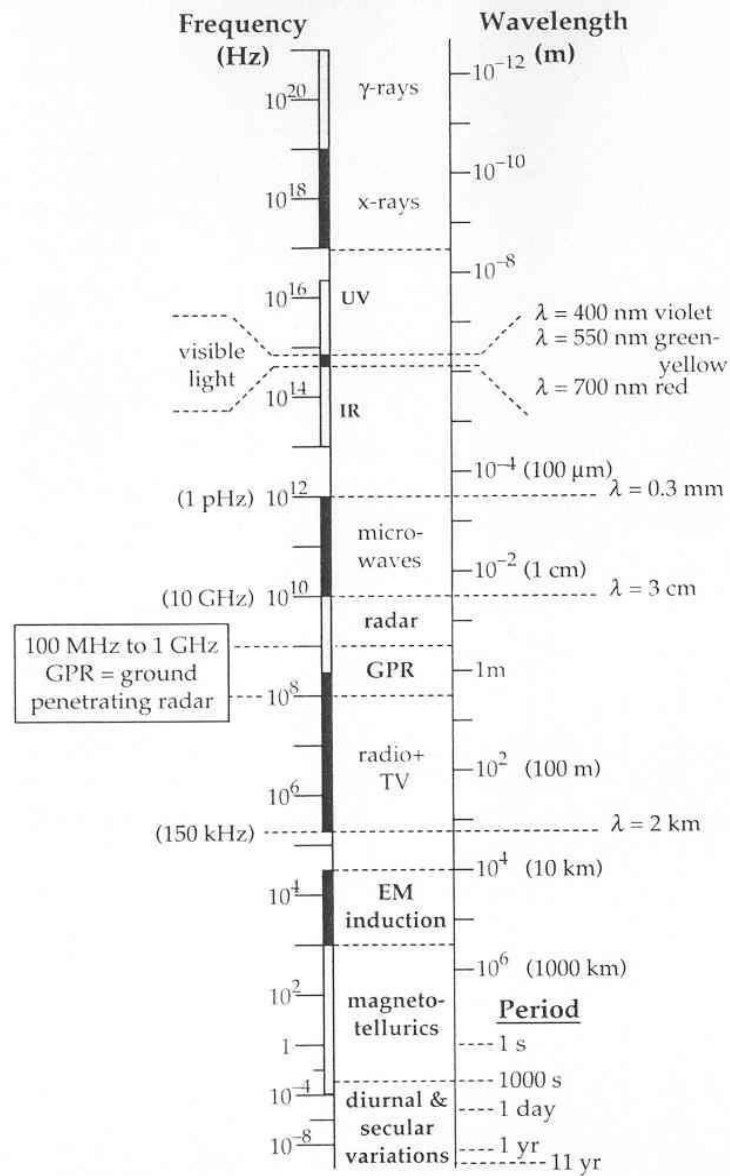


Illustration by K. Endo, Nikkei Science Inc. - Japan

Magnetosphere of the Earth is formed by the interaction of solar wind and the magnetic field of the Earth



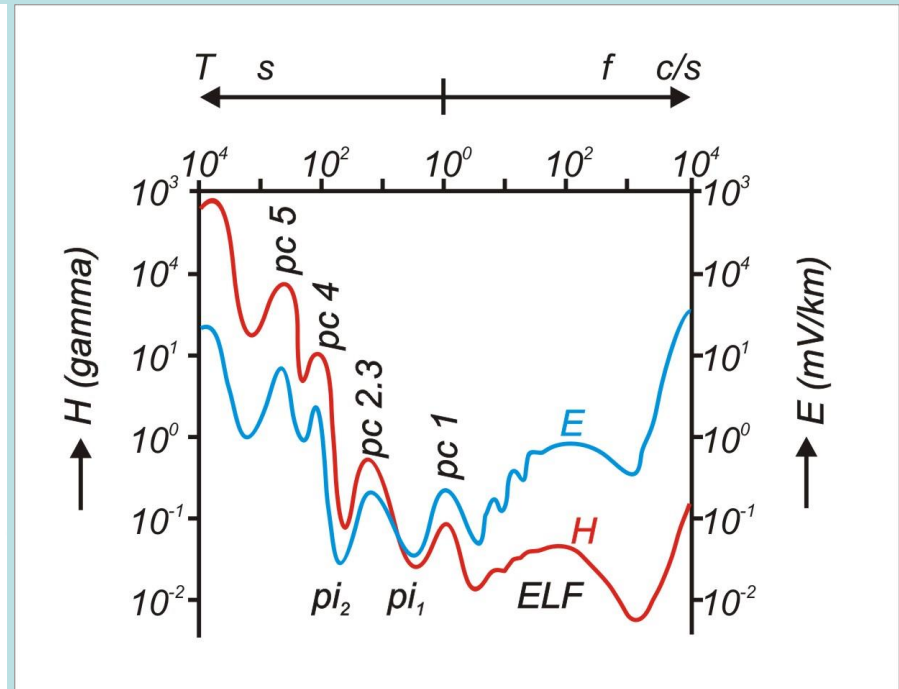
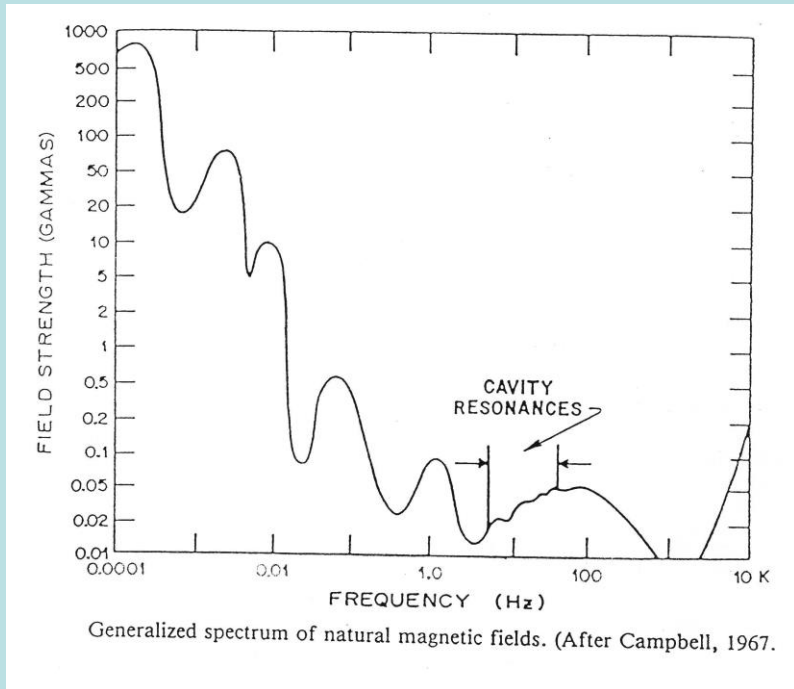
The asymmetrical form of the external magnetic field is developed by the solar wind (plasma) interacting with the magnetic field of the Earth. On the day side where the solar wind collides with the upper atmosphere the shock front (bow shock) forms. In the magnetosheath the solar wind has been slowed down and diverted around the Earth. The electrical currents due to these charged particles produce the interplanetary magnetic field which compresses the geomagnetic field on the day side and stretches it out on the night side of the Earth. A geomagnetic tail forms on the side opposite to the Sun. The magnetosheath plasma flows around the magnetopause. The magnetopause is the layer that shields the Earth environment from the solar wind.



The electromagnetic spectrum, showing the frequency and wavelength ranges of some common phenomena and the frequencies and periods used in electromagnetic surveying

Lowrie, 2007

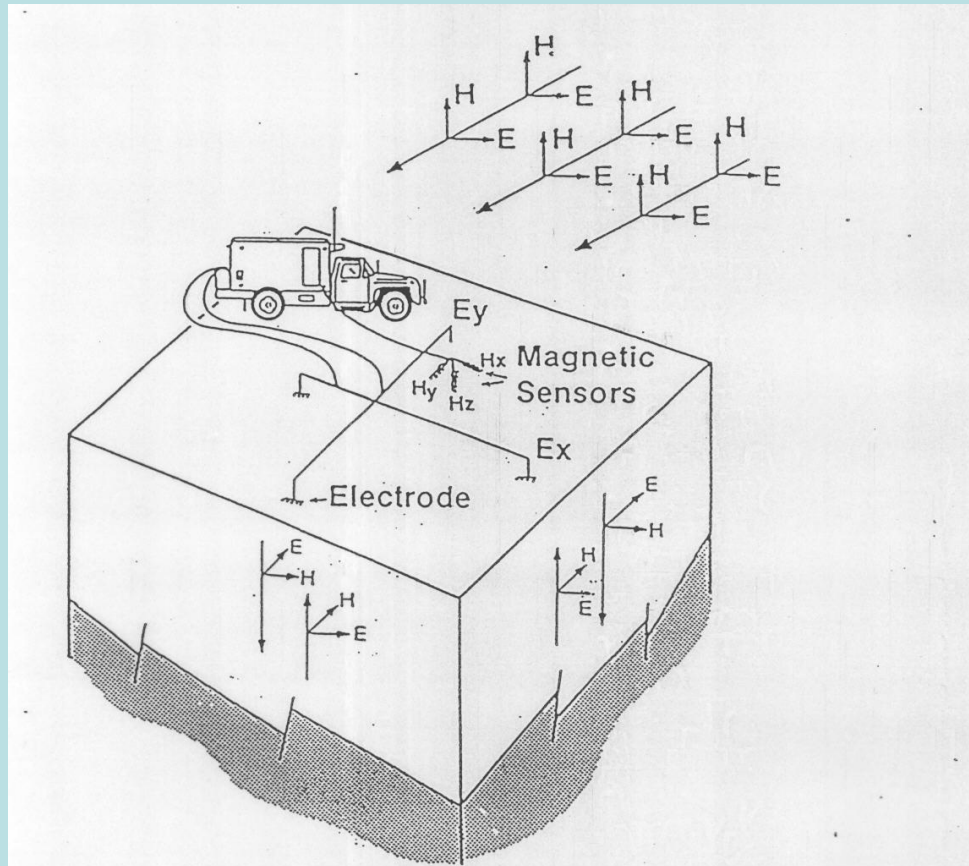
MT (magnetotellurics)



There are a set of spectrum peaks in the extremely low frequency (ELF) portion of the Earth's electromagnetic field spectrum. Schumann resonances are global electromagnetic resonances, excited by lightning discharges in the cavity formed by the Earth's surface and the ionosphere. 7.83, 14.3, 20.8, 27.3 and 33.8 Hz. (3-69Hz)

(Wikipedia)

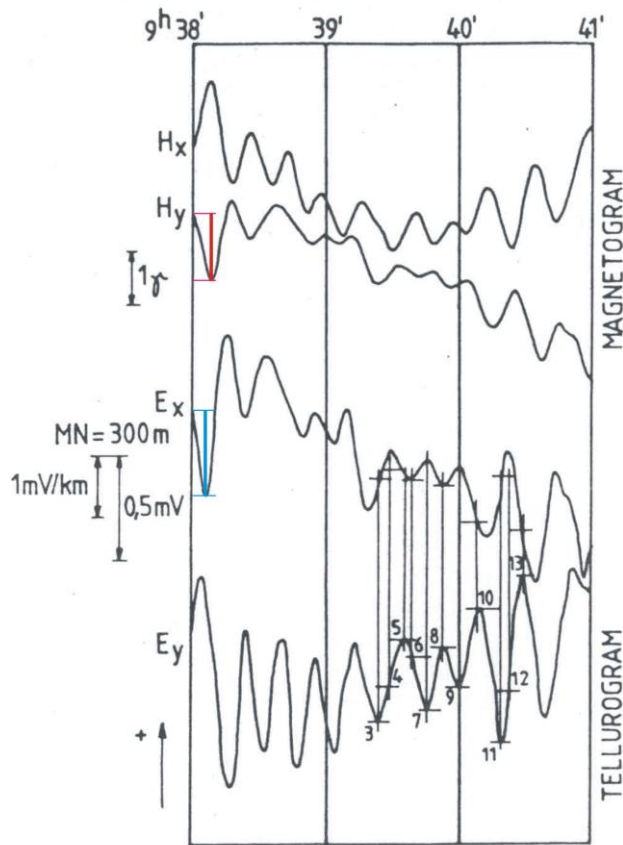
MT (magnetotellurics)



Apparent resistivity can be measured in the knowledge of the EM field components perpendicular to each other.

$$\rho = \frac{T}{2\pi\mu_o} \left(\frac{|E_{xo}|}{|H_{yo}|} \right)^2$$

MT (magnetotellurics)



Apparent resistivity can be determined as:

$$\rho = \frac{T}{2\pi\mu_o} \left(\frac{|E_{xo}|}{|H_{yo}|} \right)^2$$

$$\Delta \vec{E} + (-i\omega\mu\sigma)\vec{E} = \Delta \vec{E} + k^2 \vec{E} = \vec{0} \quad \text{If we assume only } E_x$$

$$E_x(z, t) = E_{xo} e^{-ikz} e^{i\omega t} = E_{xo} e^{-i\alpha z} e^{-\beta z} e^{i\omega t}$$

$$k = \alpha - i\beta$$

$$k^2 = \alpha^2 - 2i\alpha\beta - \beta^2 = -i\omega\mu\sigma$$

$$k = (-i\omega\mu\sigma)^{\frac{1}{2}}$$

$$\alpha = \beta = \left[\frac{\omega\mu\sigma}{2} \right]^{\frac{1}{2}}$$

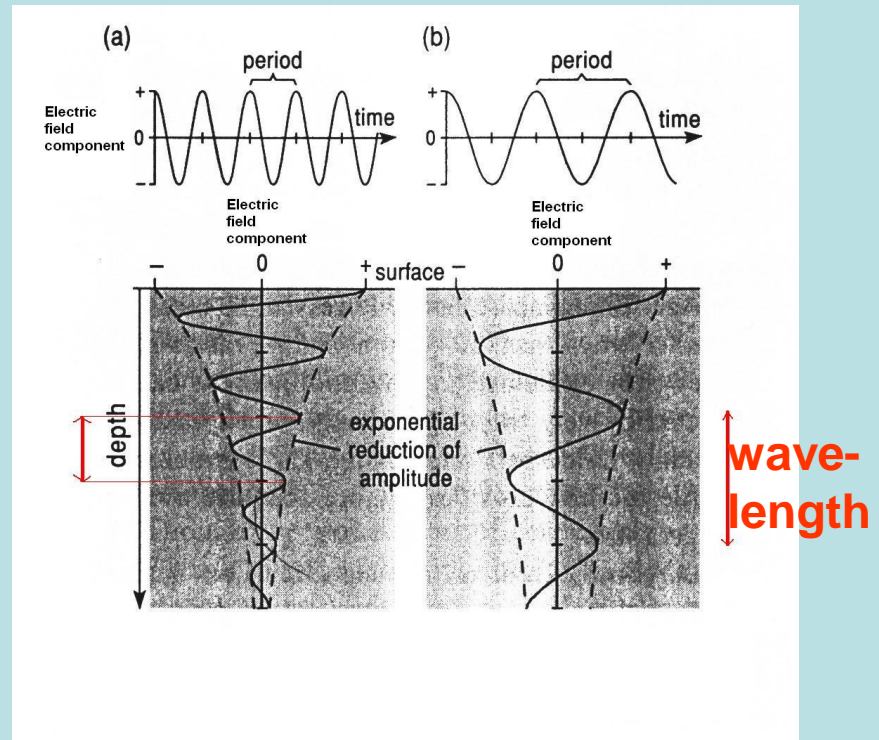
$$E_x(z, t) = E_{xo} e^{-ikz} e^{i\omega t} = E_{xo} e^{-\beta z} e^{-i\alpha z} e^{i\omega t} = E_{xo} e^{-\left[\frac{\omega\mu\sigma}{2} \right]^{\frac{1}{2}} z} e^{-\left[\frac{\omega\mu\sigma}{2} \right]^{\frac{1}{2}} iz} e^{i\omega t}$$

Skin depth is the depth at which the amplitude of a plane wave has been attenuated to 1/e

$$E_{xo} e^{-\beta z_s} = E_{xo} e^{-1}$$

$$z_s = \frac{1}{\beta} = \left[\frac{2}{\omega\mu\sigma} \right]^{\frac{1}{2}}$$

If we want to increase the exploration depth, we have to investigate the EM fields of low frequencies.



$$E_x(z, t) = E_{xo} e^{-ikz} e^{i\omega t} = E_{xo} e^{-\beta z} e^{-i\alpha z} e^{i\omega t} = E_{xo} e^{-\left[\frac{\omega\mu\sigma}{2}\right]^{1/2} z} e^{-\left[\frac{\omega\mu\sigma}{2}\right]^{1/2} iz} e^{i\omega t}$$

Wavelength is the distance over which the wave's shape repeats

$$e^{-2\pi i} = e^{-\alpha \lambda i}$$

This term determines the phase

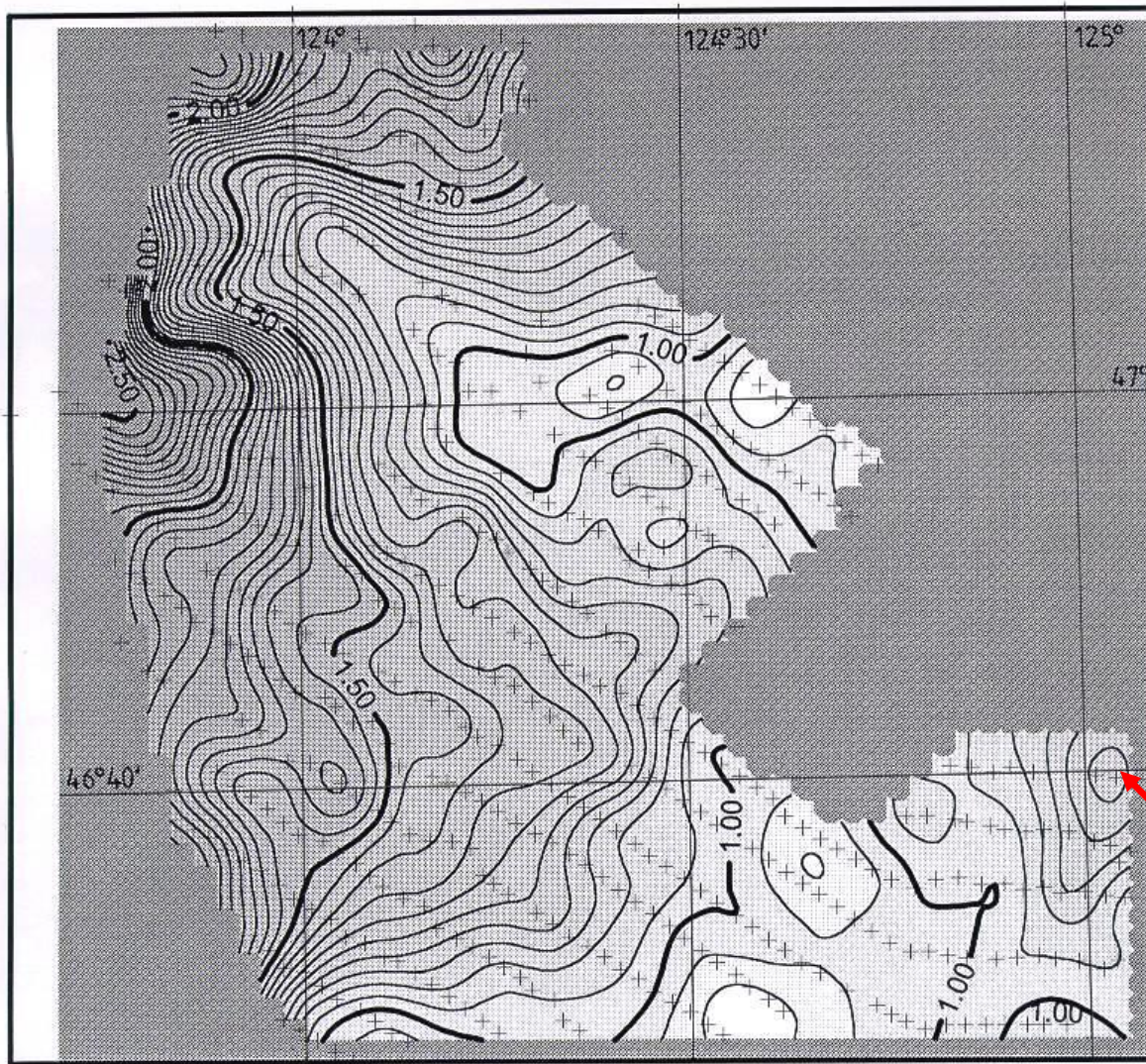
$$\lambda = 2\pi / \alpha = 2\pi \left[\frac{2}{\omega\mu\sigma} \right]^{1/2}$$

$$\alpha = \beta = \left[\frac{\omega\mu\sigma}{2} \right]^{1/2}$$

$$r \gg \lambda$$

$$r \approx \lambda$$

$$r \ll \lambda$$



Isoarea contour map reflecting basement relief changes in Daqing (China).

The less the isoarea value is the deeper the basement depth must be.

There is a depression from NW to SE.

anticline

Takács

MT (magnetotellurics)

Information
on the
lower layer

Information on
the upper layer

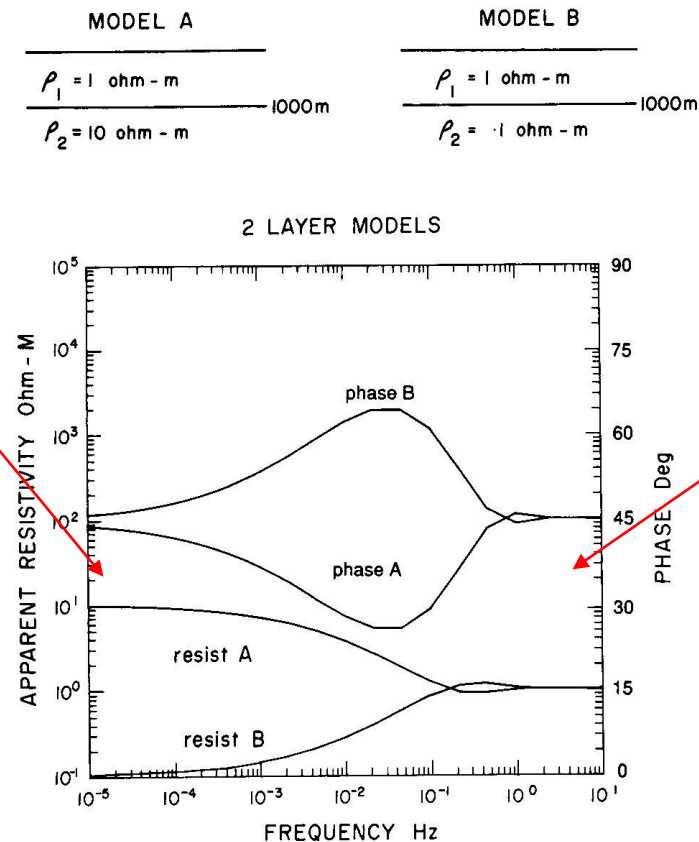
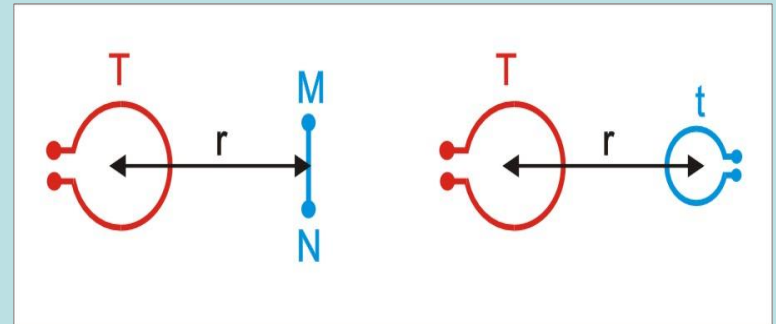
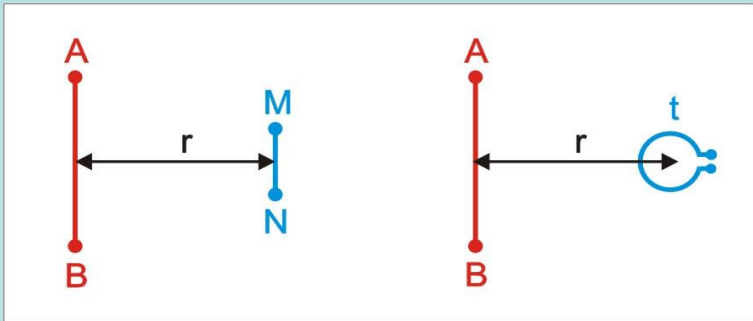


Fig. 23. MT apparent resistivity and phase responses of two-layer models. Model A—resistive basement. Model B—conductive basement.

Nabighien, 1987

Controlled source methods



Partially controlled source method: VLF

FEM methods

$$z_s = \left[\frac{2}{\omega \mu \sigma} \right]^{\frac{1}{2}} = 503.3 \sqrt{\rho T}$$

$$\lambda = 2\pi z_s$$

$$r \gg \lambda$$

Far field zone

$$r \approx \lambda$$

Transition zone

$$r \ll \lambda$$

Near field zone

z_s : skin depth at which the amplitude of a plane wave has been attenuated to $1/e$

CSAMT (controlled source audio-frequency magnetotellurics)

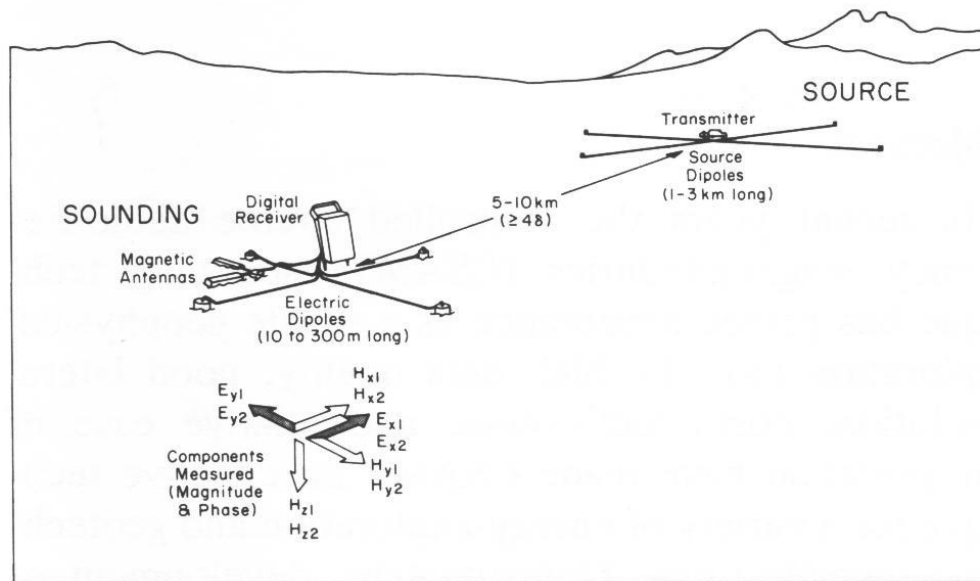


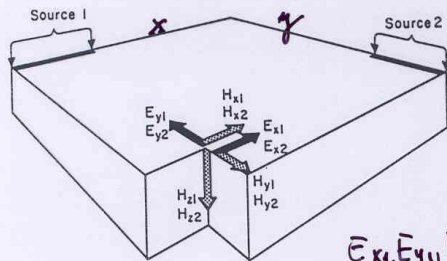
Fig. 1. Field set-up for a tensor CSAMT survey, which measures five electric and magnetic field components from two source polarizations. A common variation is scalar CSAMT, which measures E_x and H_y from a single source. In some circumstances loop sources may be used instead of a grounded dipole.

This method works in the far field zone. The same equation holds, which is used in MT:

$$\rho = \frac{T}{2\pi\mu_o} \left(\frac{|E_{xo}|}{|H_{yo}|} \right)^2$$

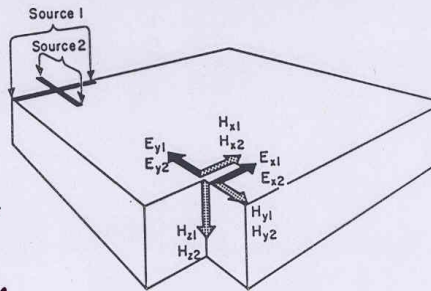
Nabighien, 1987

(a) Tensor CSAMT, Separated Sources

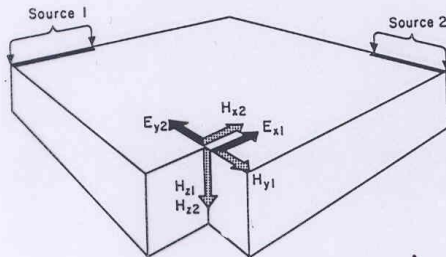


$$\begin{aligned} &E_{x1}, E_{y1}, H_{x1}, H_{y1}, H_{z1} \\ &E_{x2}, E_{y2}, H_{x2}, H_{y2}, H_{z2} \end{aligned}$$

(b) Tensor CSAMT, Coincident Sources

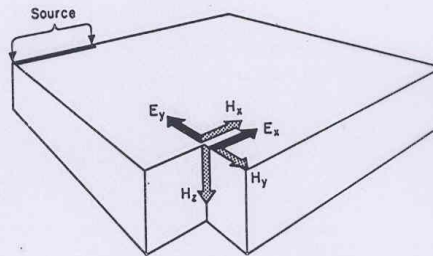


(c) Partial-Tensor CSAMT, Separated Sources



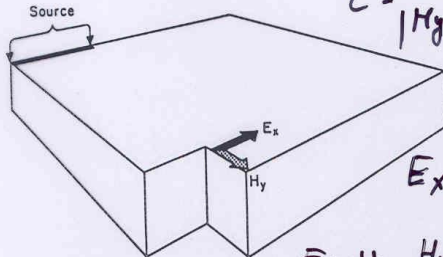
$$\begin{aligned} &E_{x1}, H_{y1}, H_{z1} \text{ or 1. formation} \\ &E_{y2}, H_{x2}, H_{z2} \text{ or 2. formation} \end{aligned}$$

(d) Vector CSAMT



$$E_x, E_y, H_x, H_y, H_z \text{ (any formation, any source)}$$

(e) Scalar CSAMT

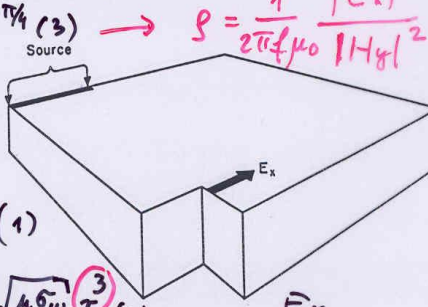


$$Z = \frac{|E_x|}{|H_y|} = \sqrt{\mu \rho \omega} \rightarrow \rho = \frac{1}{2\pi f \mu_0} \frac{|E_x|^2}{|H_y|^2}$$

$$E_x = \frac{I dl}{\pi \sigma r^3} \quad (1)$$

$$E_x, H_y \quad H_y = I dl / \pi \sqrt{\mu \sigma \omega} r^3 \quad (2)$$

(f) Scalar CSAET

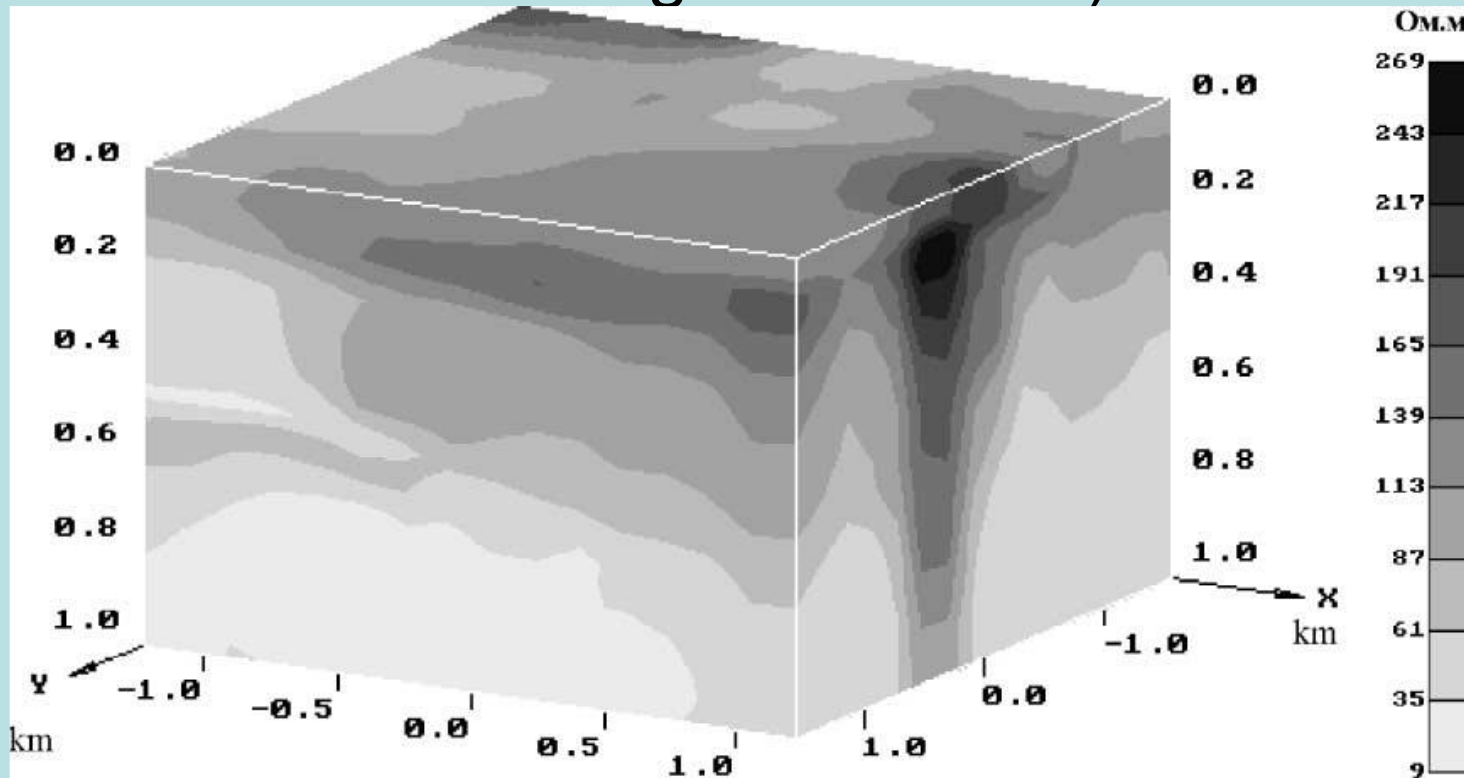


CSAMT ARRAYS.

The most simple ones are scalar measurements, the most complicated ones are tensor measurements.

The resistivity does not have any transmitter-receiver distance in the far field zone.

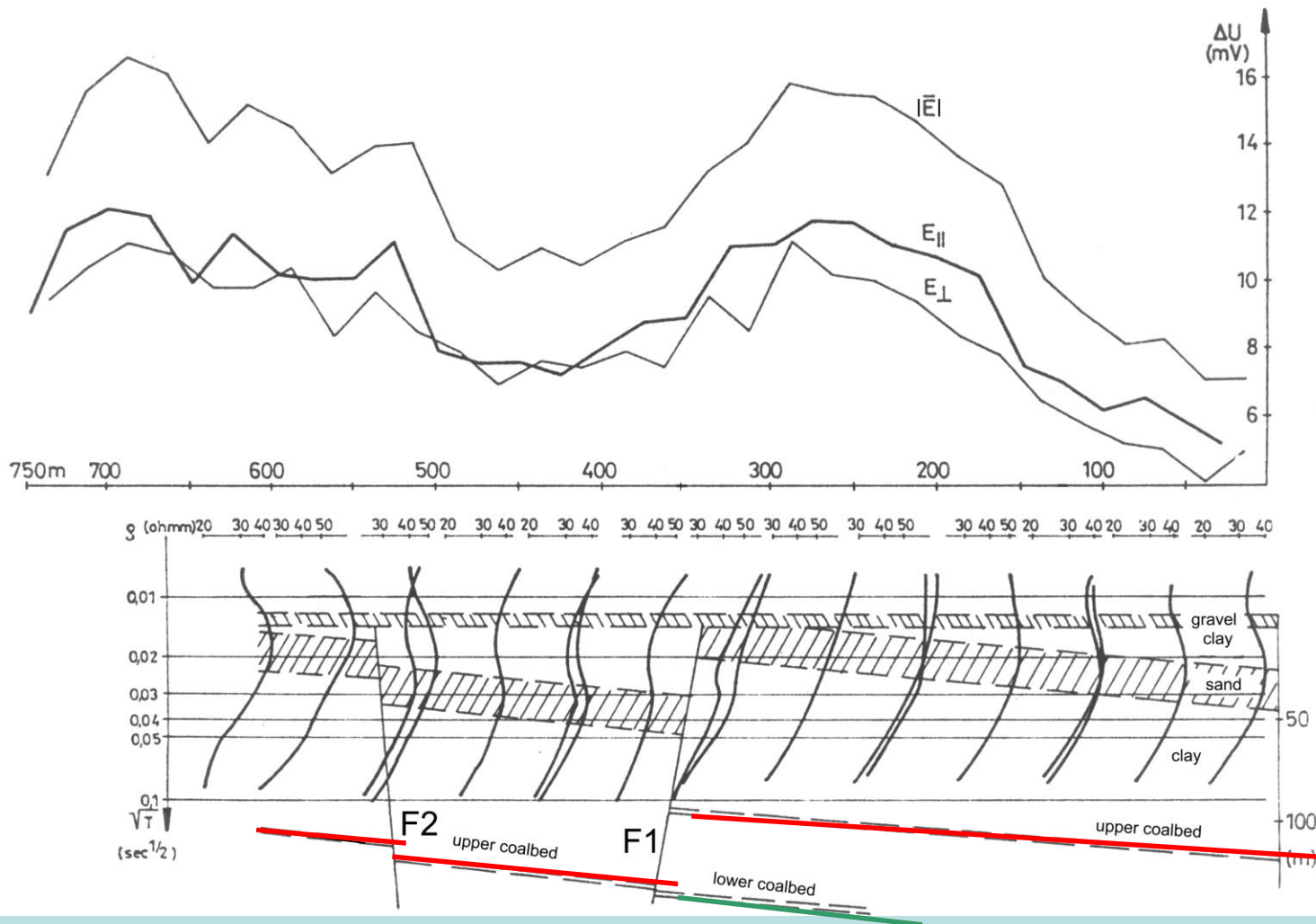
CSAMT (controlled source audio-frequency magnetotellurics)



Bostick resistivity cube, it yields the resistivity distribution in the function of depth. Besides the slope of the resistivity response the skin depth-conductivity relationship (valid in MT for homogeneous half-space) is used, however, app.resistivity is substituted into the equation Spichak et. al. 2002.

$$z_s = \frac{1}{\beta} = \left[\frac{2}{\pi \mu \sigma} \right]^{\frac{1}{2}}$$

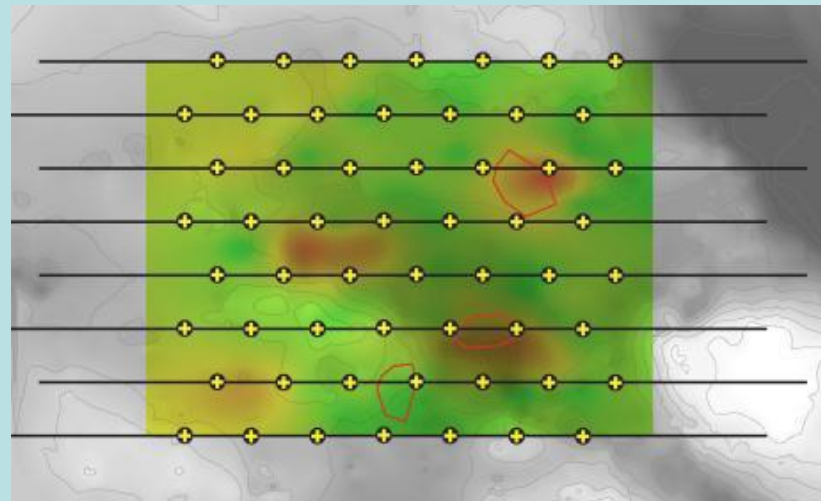
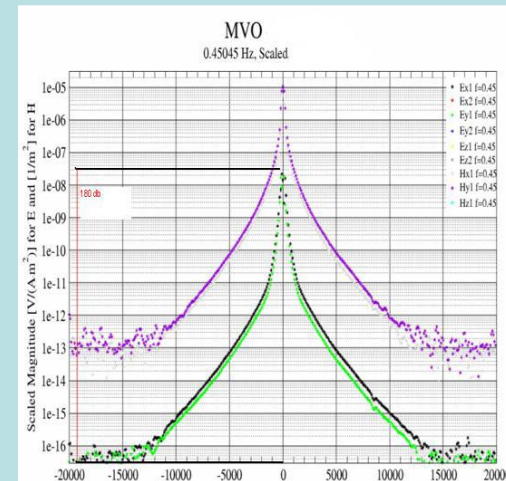
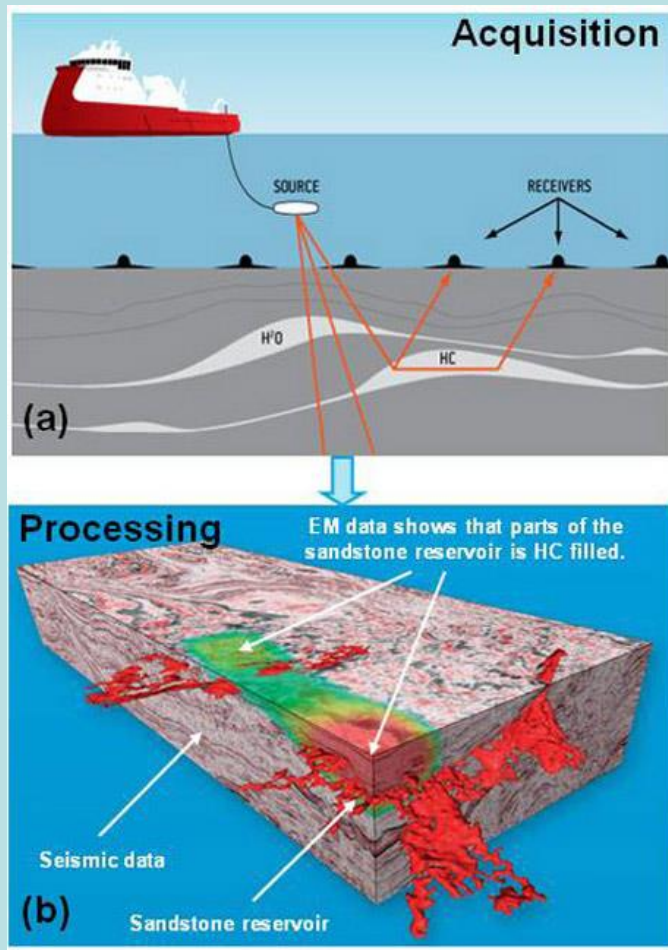
BORSOD COUNTY TRANSITION ZONE MEASUREMENT



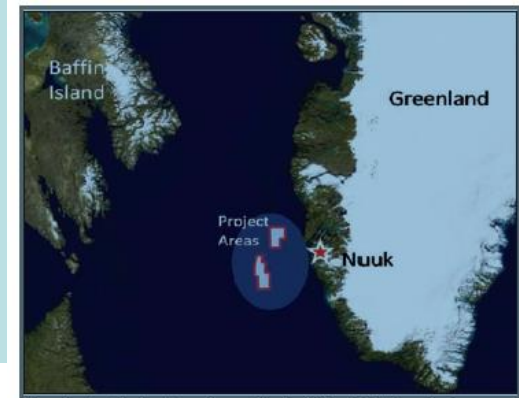
The task was to determine coalbeds depth variation. Instead of it the depth position of the younger and thicker sand layer closer to the surface was followed. It can be accepted, because the faults caused similar vertical displacement both in the younger layers and in older coalbeds.

CSEM (controlled source electromagnetics)

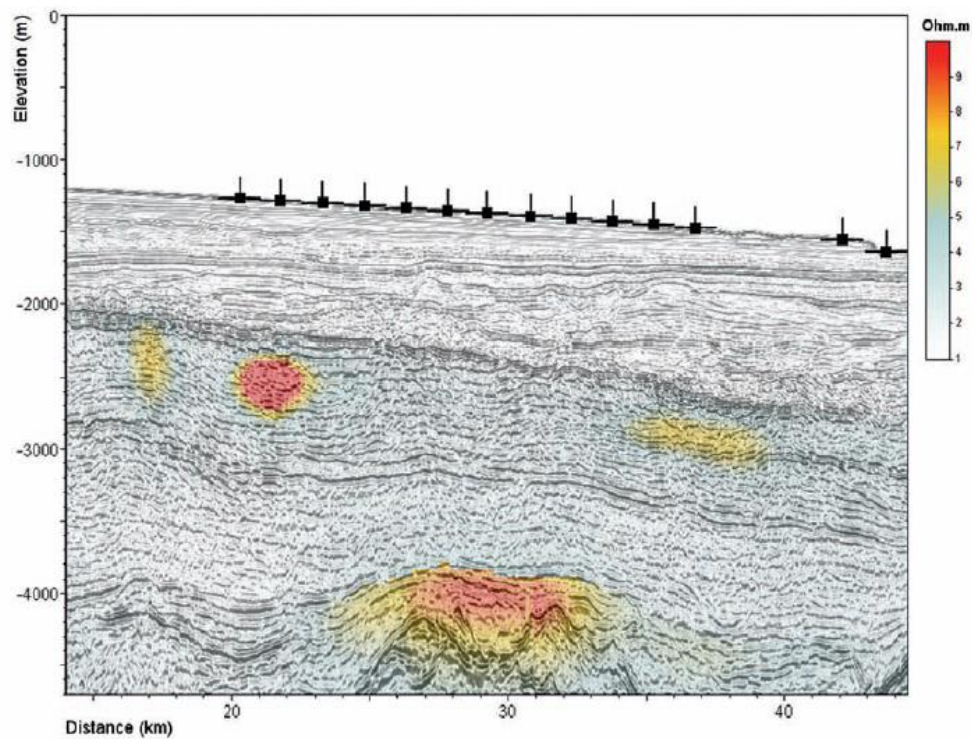
MCSEM (marine controlled source electromagnetics)



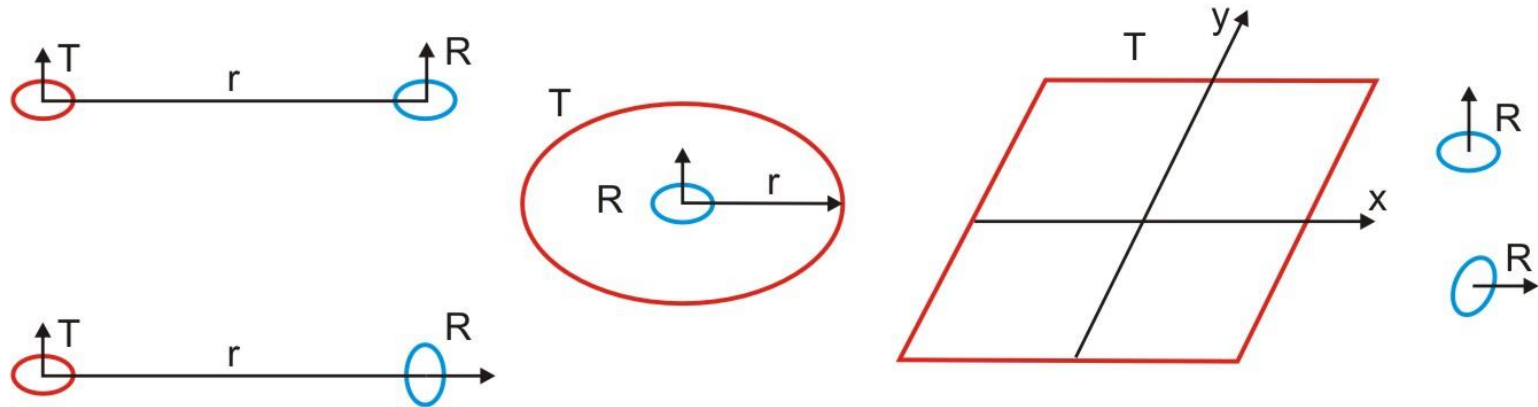
CSEM application



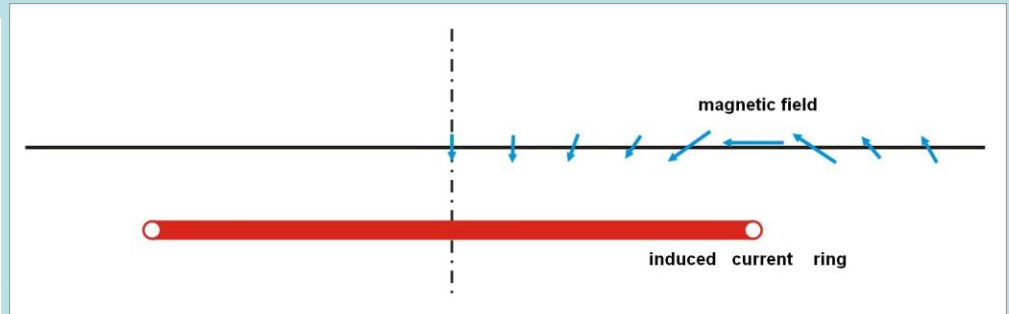
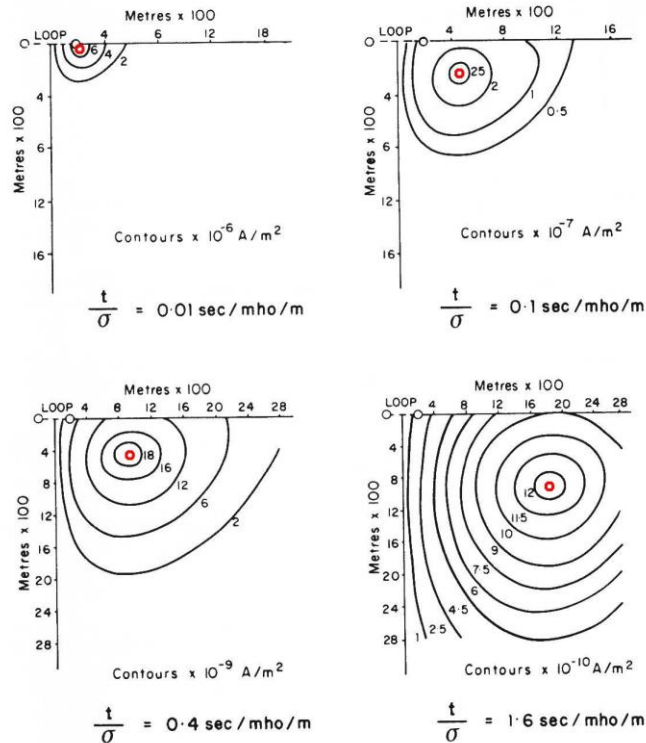
Map showing the location of survey blocks offshore West Greenland.



Transient EM methods



Transient EM methods

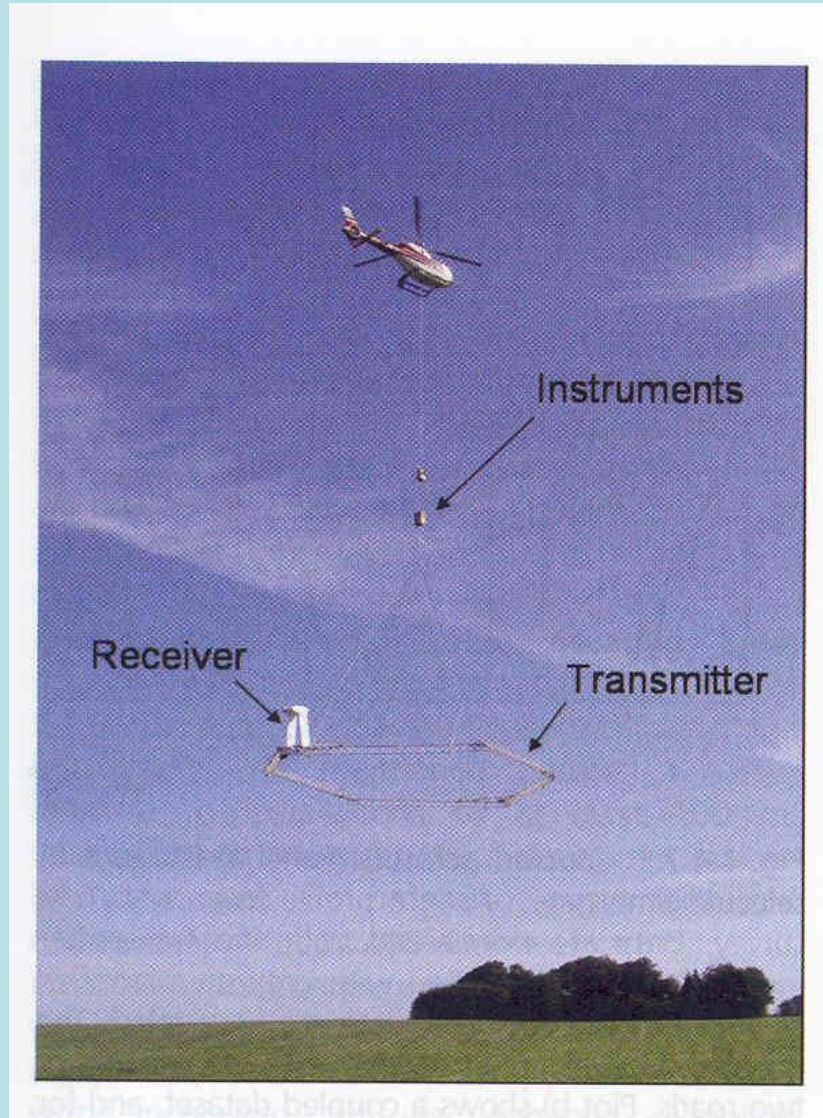


After switching off immediately a surface current flows, distributed in such a way as to maintain the magnetic field everywhere at the value that existed before turn-off. Later the current appears to have moved out and down as a diffusing current ring.

SNAPS about the position of the induced current ring. The larger the elapsed time is, the deeper the induced current penetrates (on the left, based on Geonics Ltd).

Exactly over the induced current ring the magnetic field is horizontal (above).

Transient EM methods



Comparison between FEM AND TEM methods

$$z_s = \left[\frac{2}{\omega \mu \sigma} \right]^{\frac{1}{2}} = 503.3 \sqrt{\rho T}$$

$$\lambda = 2\pi z_s$$

$$\delta = \left[\frac{2t}{\mu \sigma} \right]^{\frac{1}{2}} = 1262 \sqrt{\rho t}$$

$$d = 2\pi \delta$$

$$r \gg \lambda$$

Far field zone

$$r \approx \lambda$$

Transition zone

$$r \ll \lambda$$

Near field zone

$$r \gg d$$

$$r \approx d$$

$$r \ll d$$

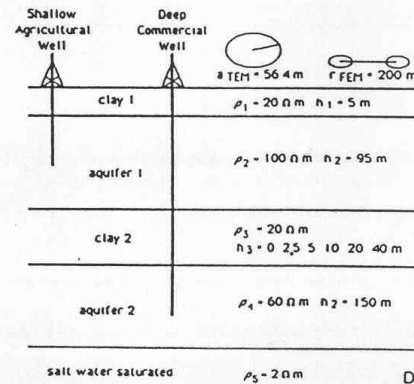
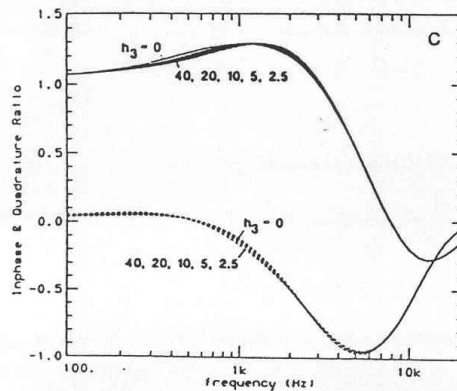
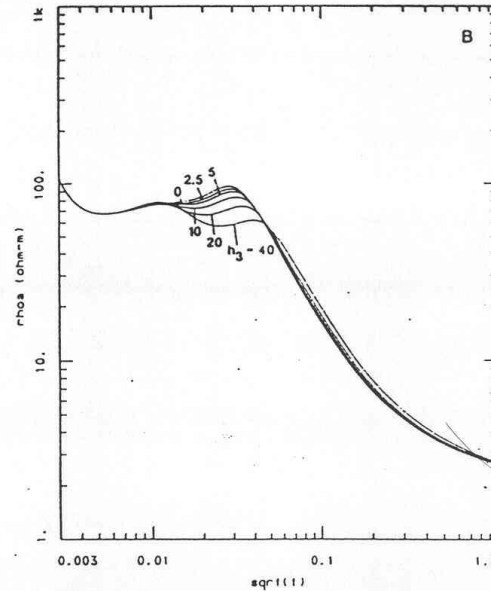
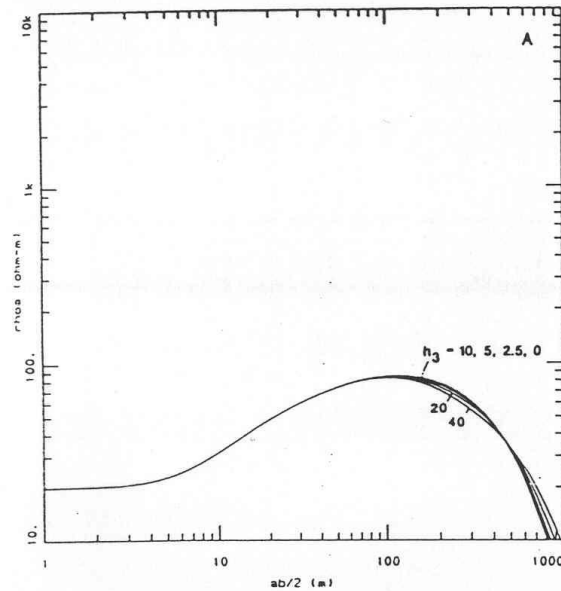
z_s

skin depth at which the
amplitude of a plane wave
has been attenuated to 1/e

δ

is the diffusion depth in
case of time domain
method

TEM method : transient electromagnetics, timedomain EM method



TNO report
Delft

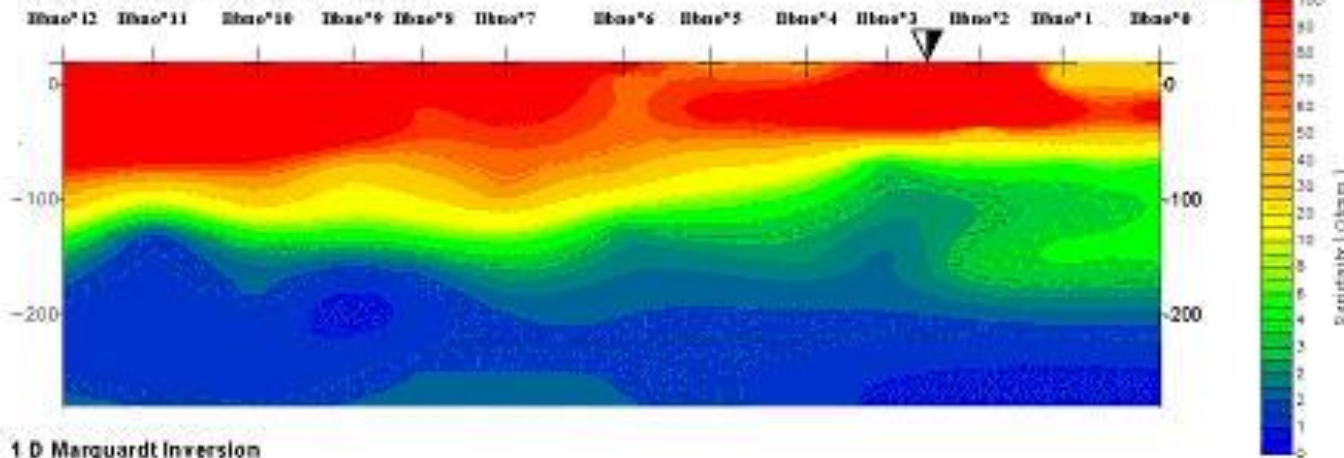
Transient EM methods, case history

Batabano, Cuba 1988

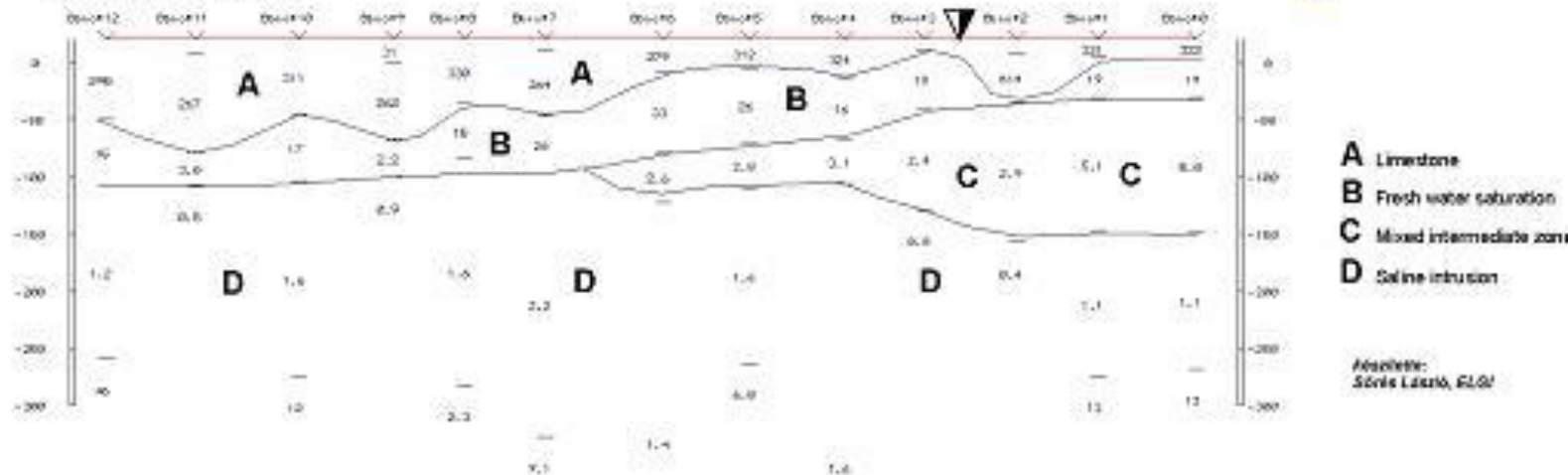
Time Domain EM Profile

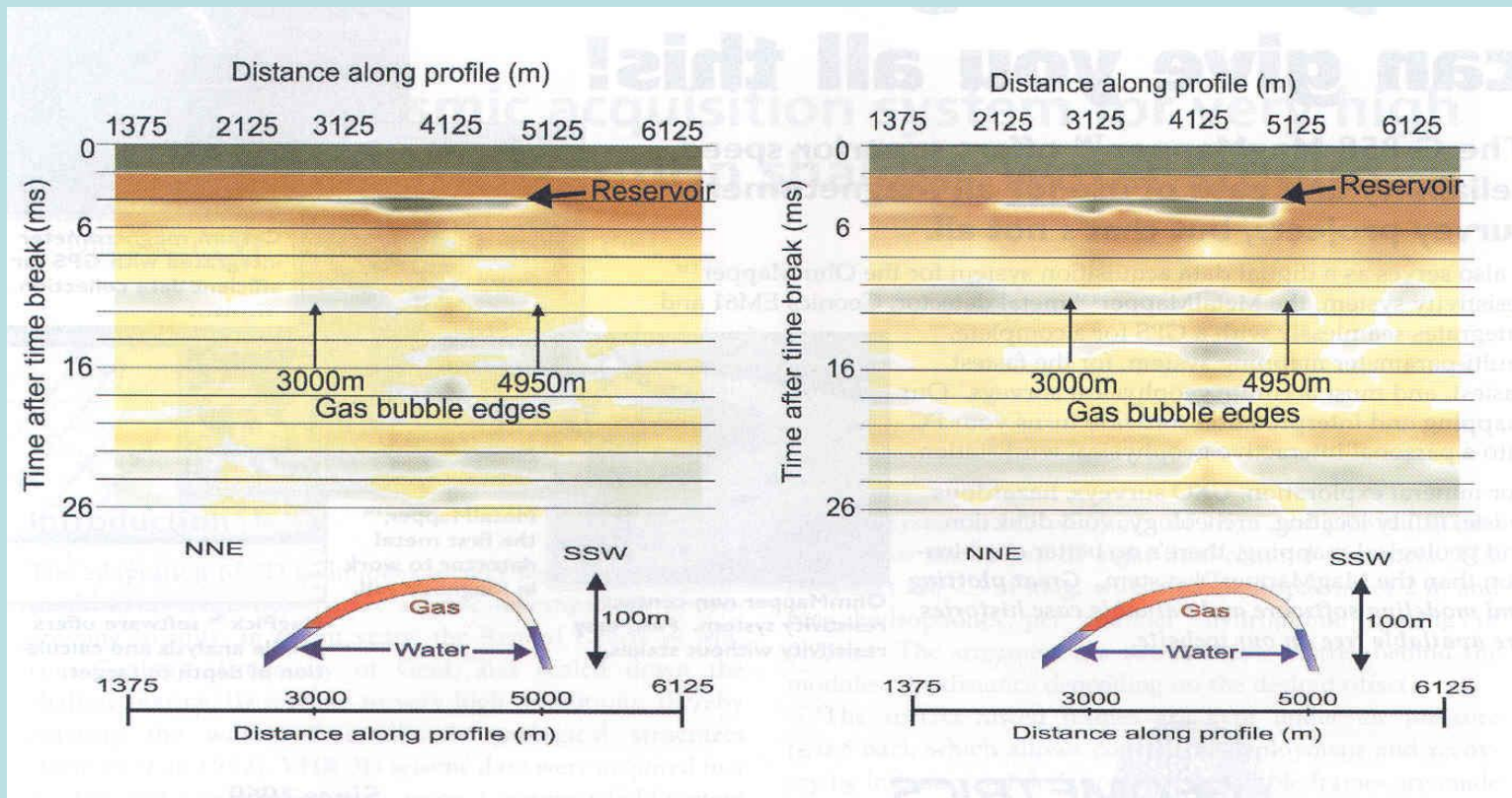
Color Image of Smooth Inversion Data

Water pumps



1 D Marquardt Inversion





TEM monitoring over a gas reservoir in Paris Basin after Ziolkowsky et. al. (2002). The measurement was repeated after two years. The changes in the saturations can be monitored, because the produced gas was replaced by water.

GEORADAR (GPR GROUND PENETRATING RADAR)

Theoretical aspects

$$\Delta \vec{E} + (\mu \varepsilon \varpi^2 - i \varpi \mu \sigma) \vec{E} = \Delta \vec{E} + k^2 \vec{E} = \vec{0}$$

$$E_x(z, t) = E_{x0} e^{-ikz} e^{i\varpi t} = E_{x0} e^{-i\alpha z} e^{-\beta z} e^{i\varpi t} \quad k = \alpha - i\beta$$

$$k^2 = \alpha^2 - 2i\alpha\beta - \beta^2 = \mu \varepsilon \varpi^2 - i \varpi \mu \sigma$$

$$\alpha = \varpi \left\{ \frac{\mu \varepsilon}{2} \left[\left(1 + \frac{\sigma^2}{\varepsilon^2 \varpi^2} \right)^{\frac{1}{2}} + 1 \right] \right\}^{\frac{1}{2}} \quad \beta = \varpi \left\{ \frac{\mu \varepsilon}{2} \left[\left(1 + \frac{\sigma^2}{\varepsilon^2 \varpi^2} \right)^{\frac{1}{2}} - 1 \right] \right\}^{\frac{1}{2}}$$

Skin depth and wavelength in general case

$$E_{xo} e^{-\beta z_s} = E_{xo} e^{-1}$$

$$z_s = 1/\beta = 1/\varpi \left\{ \frac{\mu\varepsilon}{2} \left[\left(1 + \frac{\sigma^2}{\varepsilon^2 \varpi^2} \right)^{\frac{1}{2}} - 1 \right] \right\}^{\frac{1}{2}}$$

$$e^{-2\pi i} = e^{-\alpha \lambda i}$$

$$\lambda = 2\pi/\alpha = 2\pi/\varpi \left\{ \frac{\mu\varepsilon}{2} \left[\left(1 + \frac{\sigma^2}{\varepsilon^2 \varpi^2} \right)^{\frac{1}{2}} + 1 \right] \right\}^{\frac{1}{2}}$$

The velocity and wavelength of EM wave

$$v = \lambda / T = \lambda f$$

MT, VLF etc.

$$v = \lambda / T = 2\pi \left[\frac{f}{\pi \mu \sigma} \right]^{\frac{1}{2}}$$

$$\lambda = 2\pi / \alpha = 2\pi \left[\frac{2}{\omega \mu \sigma} \right]^{\frac{1}{2}}$$

General case

$$v = 1 / \left\{ \frac{\mu \epsilon}{2} \left[\left(1 + \frac{\sigma^2}{\epsilon^2 \omega^2} \right)^{\frac{1}{2}} + 1 \right] \right\}^{\frac{1}{2}}$$

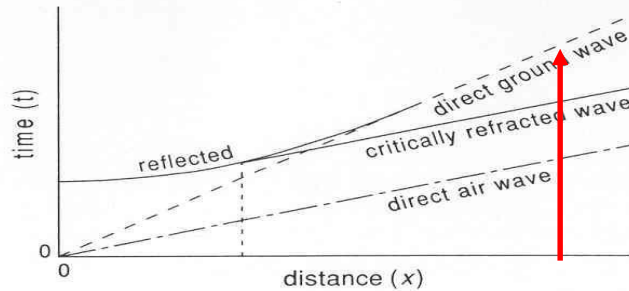
$$\lambda = 2\pi / \alpha = 2\pi / \omega \left\{ \frac{\mu \epsilon}{2} \left[\left(1 + \frac{\sigma^2}{\epsilon^2 \omega^2} \right)^{\frac{1}{2}} + 1 \right] \right\}^{\frac{1}{2}}$$

If displacement current is dominant over conduction current

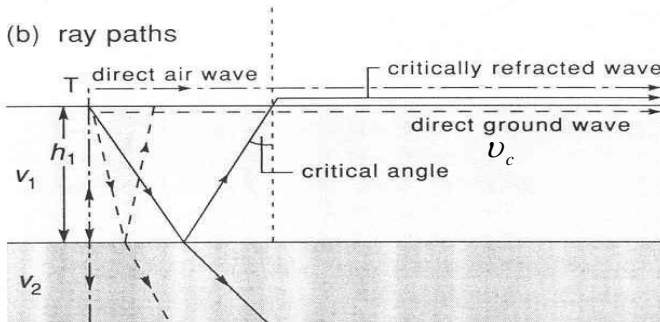
$$v = \frac{1}{\sqrt{\mu \epsilon}} = \frac{1}{\sqrt{\mu_o \epsilon_o \epsilon_r}} = \frac{c}{\sqrt{\epsilon_r}}$$

$$\lambda = 2\pi / \alpha = 2\pi / \sqrt{\mu \epsilon \omega^2} = \frac{1}{f \sqrt{\mu \epsilon}} = \frac{v}{f}$$

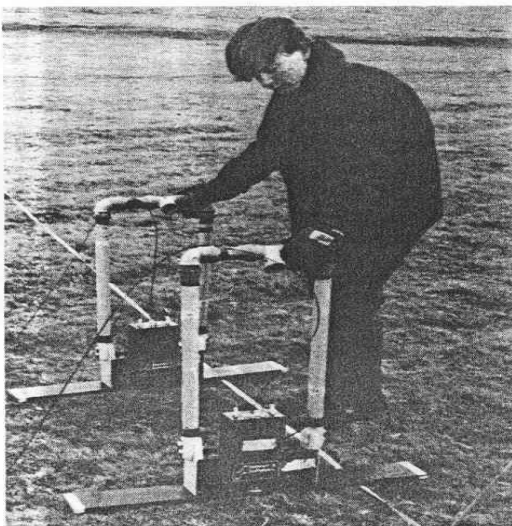
(a) time–distance graph



(b) ray paths



(c) Pulse EKKO IV ground-penetrating radar



Within the critical distance ($2htg\nu_c$) we can record only three waves' arrival.

If the offset is larger than this distance is, there are four waves:

- 1. direct air wave**
- 2. critically refracted wave**
- 3. direct ground wave**
- 4. reflected wave**

$$\sin \nu_c = \frac{v_1}{v_{air}}$$

Musett & Khan, 2000

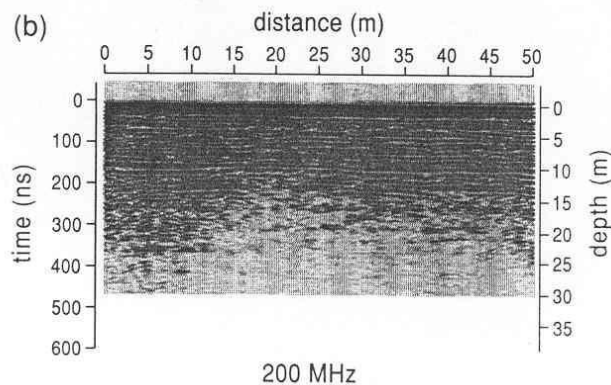
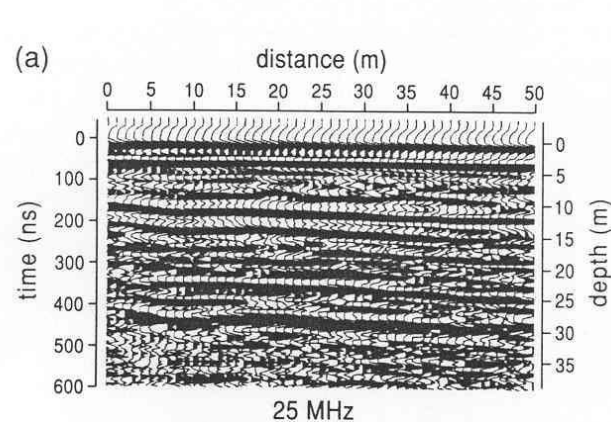
Reflection coefficient (R)

$$R = \frac{Z_2 - Z_1}{Z_2 + Z_1}$$

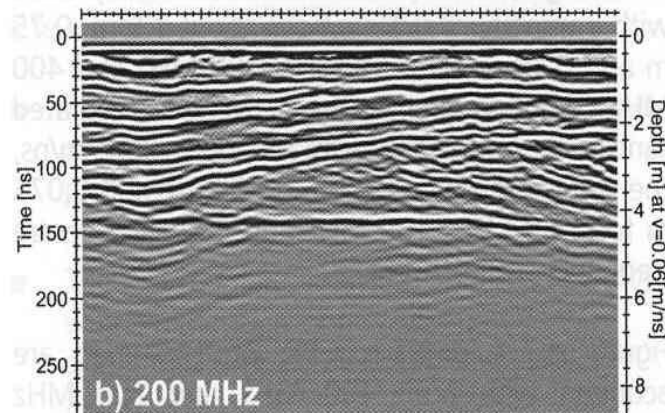
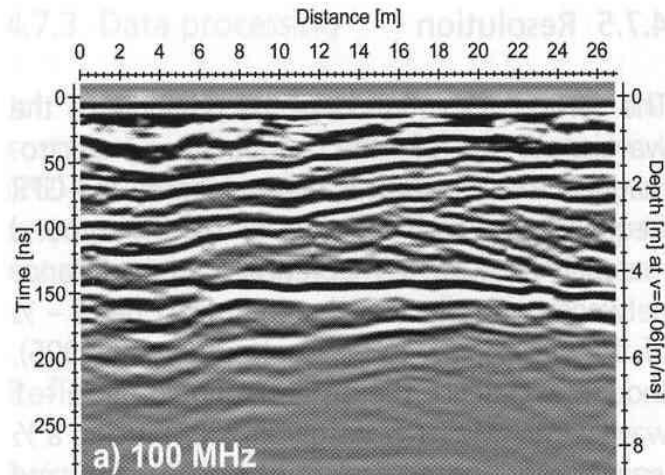
$$R = \frac{\frac{\omega\mu_2}{k_2} - \frac{\omega\mu_1}{k_1}}{\frac{\omega\mu_2}{k_2} + \frac{\omega\mu_1}{k_1}} \approx \frac{\sqrt{\epsilon_{r1}} - \sqrt{\epsilon_{r2}}}{\sqrt{\epsilon_{r1}} + \sqrt{\epsilon_{r2}}}$$

Material	ϵ_r	V (m/ns)
Dry sand/gravel	4-10	0.15-0.09
Wet sand/gravel	10-20	0.09-0.07
Dry clay/silt	3-6	0.17-0.12
Wet clay/silt	7-40	0.11-0.05
Cement (dry/wet)	6-11	0.12-0.09
Granite	4-9	0.15-0.10
Limestone	4-8	0.15-0.11
Dry salt	5-6	0.13-0.12
Permafrost	4-5	0.15-0.13
Glacier ice	3.5	0.16
Fresh water	81	0.03
Methyl alcohol	31	0.05
Petroleum/Kerosene	2.1	0.20
Aviation gasoline	1.95	0.21
Air	1	0.30

Sharma 1997



The same GPR section at two frequencies.



The greater the frequency is, the higher the attenuation and better the resolution will be. Mussett et. al. 2000; BurVal Working Group, 2006

Questions

- What do you know about the change of direction of a current flow if it crosses a boundary?
- Characterize Wenner, Schlumberger and a dipole-dipole array.
- What is the aim of a VES measurement, what is the essence of the S-type equivalence?
- What is the difference between IP method in time and in frequency domain?
- How can you classify the EM methods?
- What is the essence of MT methods?
- What do you mean by skin-depth?
- What is the essence of CSAMT method?
- What do you mean by in-phase and out-of-phase EM component?
- Which are the main application fields of FEM methods?
- What is the essence of the Bostick transformation?
- What do you know about the physical principle of transient EM method?
- When can you suggest the application of transient method?